GENIORS

Research and Innovation Action (RIA)

This project has received funding from the European Union's Horizon 2020 research and innovation programme under grant agreement No 755171.

Start date : 2017-06-01 Duration : 48 Months
http://geniors.eu/

Status on Distribution data and chemical modelling

Authors : Mr. Andreas GEIST (KIT), Maximilian Henkes (JUELICH), Irena Herdzik-Koniecko (ICHTJ), Fabian Kreft (JUELICH), Giuseppe Modolo (JUELICH), Jerzy Narbutt (ICHTJ), Dimitri Schneider (JUELICH), Magdalena Rejnis-Strzelak (ICHTJ), Bart Verlinden (SCK-CEN), Patrik Wessling (KIT), Andreas Wilden (JUELICH)

GENIORS - Contract Number: 755171

Project officer: Roger Garbil

Document title	Status on Distribution data and chemical modelling
Author(s)	Mr. Andreas GEIST, Maximilian Henkes (JUELICH), Irena Herdzik-Koniecko (ICHTJ), Fabian Kreft (JUELICH), Giuseppe Modolo (JUELICH), Jerzy Narbutt (ICHTJ), Dimitri Schneider (JUELICH), Magdalena Rejnis-Strzelak (ICHTJ), Bart Verlinden (SCK-CEN), Patrik Wessling (KIT), Andreas Wilden (JUELICH)
Number of pages	36
Document type	Deliverable
Work Package	WP3
Document number	D3.2
Issued by	KIT
Date of completion	2021-02-01 16:07:44
Dissemination level	Public

Summary

To design and optimise a solvent extraction process, accurate equilibrium data and the respective equilibrium models are required to describe the distribution of key components between organic and aqueous phases. The Deliverable Report, D3.2, Status on distribution data and chemical modelling, compiles equilibrium distribution data for the extraction of actinide and lanthanide ions and of nitric acid by several solvent extraction systems developed and studied in GENIORS, ? TODGA /HNO3 ? DMDOHEMA / HNO3 ? cis-mTDDGA / HNO3 ? TODGA + DMDOHEMA / PTD in HNO3 ? cis-mTDDGA / PTD in HNO3 ? TODGA + modifiers / HNO3 ? PTEH / HNO3 Furthermore, equilibrium models for the systems TODGA /HNO3, DMDOHEMA / HNO3 and PTEH / HNO3 are reported.

Approval

Date	By
2021-02-01 17:05:16	Mr. Philippe GUILBAUD (CEA)
2021-02-01 17:25:51	Mr. Andreas GEIST (KIT)
2021-02-04 07:47:39	Mr. Stéphane BOURG (CEA)

CONTENTS

This project has received funding from the EURATOM research and training programme 2014–2018 under grant agreement No. 755171. The content of this deliverable reflects only the authors' view. The European Commission is not responsible for any use that may be made of the information it contains.

INTRODUCTION

To design and optimise a solvent extraction process, accurate equilibrium data and the respective equilibrium models are required to describe the distribution of key components between organic and aqueous phases. The Deliverable Report, *D3.2, Status on distribution data and chemical modelling,* compiles equilibrium distribution data for the extraction of actinide and lanthanide ions and of nitric acid by several solvent extraction systems developed and studied in GENIORS,

- TODGA /HNO_3
- DMDOHEMA / HNO_3
- *cis*-mTDDGA / HNO_3
- TODGA + DMDOHEMA / PTD in HNO_3
- *cis*-mTDDGA / PTD in HNO_3
- TODGA + modifiers / HNO_3
- PTEH / HNO_3

Furthermore, equilibrium models for the systems TODGA /HNO_3, DMDOHEMA / HNO_3 and PTEH / HNO_3 are reported.

TODGA

TODGA *(N,N,N',N'*-tetra-*n*-octyl diglycolamide, Figure 1)[1-3] is an efficient extracting agent for actinide and lanthanide ions. It is central to the development of actinide separation processes. TODGA based processes for co-extracting An(III) and Ln(III) from HLLW are under development in Europe (mostly in the context of EURATOM projects) and in many other countries.[4-5] TODGA is also used in the EURO-GANEX process which co-separates TRU.[6-10]

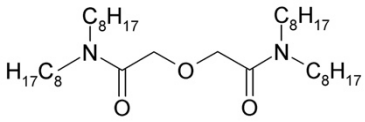

Figure 1. TODGA.

EXTRACTION OF NITRIC ACID

The extraction of nitric acid into solvents composed of TODGA dissolved in kerosene/1-octanol diluents and into the kerosene/1-octanol diluent itself was studied and modelled.[11] To this, a sophisticated model for the extraction of nitric acid into the diluent was established, based on experimental data published earlier.[12] Furthermore, a model for the extraction of nitric acid into the TODGA solvent was established. Details are given in reference.[11] The abstract from this paper is cited below:

This project has received funding from the EURATOM research and training programme 2014–2018 under grant agreement No. 755171. The content of this deliverable reflects only the authors' view. The European Commission is not responsible for any use that may be made of the information it contains.

"Distribution data for the partition of nitric acid between nitric acid solution and a solvent phase comprising various combinations of TODGA, octanol, and inert kerosene diluent have been generated, covering a range of conditions from 0 to 9 mol/L HNO_3(aq), 0–100% octanol, 0–0.4 mol/L TODGA over a temperature range from 10°C to 50°C. The data have been used to derive a model describing the nitric acid equilibrium between the phases suitable for incorporation in process models of the innovative SANEX process, for example. For the nitric acid/octanol/diluent system, it was found that an accurate prediction of nitric acid distribution could be achieved using a model allowing 1:1, 1:2, and 1:3 nitric acid/octanol adducts. For the nitric acid/TODGA/diluent system, the best models were found to be those allowing 4:1, 3:1, 2:1, 1:1, and 2:2 nitric acid/TODGA adducts. Superimposing the models for nitric acid distribution into the individual extractants and comparing with experimental results for the nitric acid/octanol/TODGA system showed systematic differences indicative of antagonistic and synergistic effects applying in the ranges 0.5–1.5 mol/L HNO_3 and > 1.5 mol/L HNO_3, respectively. These effects were modelled by the inclusion of 0:1:2, 1:1:1, 2:1:3, and 3:1:2 nitric acid/TODGA/octanol adducts. The effect of temperature on nitric acid extraction was well described by an Arrhenius type expression with an activation energy of −25.7 kJ/mol. No diluent dependence was found for nitric acid extraction."

DMDOHEMA

DMDOHEMA *(N,N'*-dimethyl-*N,N'*-dioctyl-2-[2-(hexyloxy)ethyl] malonamide, Figure 2)[13] was used in actinide separations processes developed at the CEA and in earlier EURATOM projects such as NEWPART and PARTNEW. More recently it is used in the EURO-GANEX process.

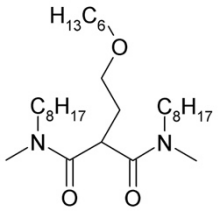

Figure 2. DMDOHEMA.

EXTRACTION OF ACTINIDES, LANTHANIDES AND NITRIC ACID

The extraction of actinides(III), lanthanides(III) and nitric acid into DMDOHEMA dissolved in kerosene was studied and equilibrium models for the extraction of nitric acid and of Am(III) were developed. Details are given in reference.[14] The abstract from this paper is cited below:

"Liquid-liquid distribution data were determined for the extraction of nitric acid, Am(III), Cm(III), and lanthanides(III) from 0.1–7 mol/L nitric acid into 0.5–1 mol/L N,N'-dimethyl-N,N'-dioctyl-2-[2-(hexyloxy)ethyl]-malonamide (DMDOHEMA) dissolved in kerosene. Nitric acid extraction was accurately modeled accounting for the adducts $(HNO_3)L_2$, $(HNO_3)L$, and $(HNO_3)_2L$. To model Am(III) extraction, the following complexes were taken into account, $Am(NO_3)_3L_4$, $Am(NO_3)_3(HNO_3)L_3$, and a third complex, $Am(NO_3)_3(HNO_3)_2\mathbf{L_3}$ (considering spectroscopic results) or $Am(NO_3)_3(HNO_3)_2\mathbf{L_2}$

This project has received funding from the EURATOM research and training programme 2014–2018 under grant agreement No. 755171. The content of this deliverable reflects only the authors' view. The European Commission is not responsible for any use that may be made of the information it contains.

(considering slope-analysis results). Separation factors for Am(III) over Cm(III) and the lighter lanthanides(III) are practically independent of nitric acid concentration. Am(III)/Ln(III) separation factors decrease with increasing nitric acid concentration for the heavier lanthanides(III).”

IMPROVING THE EURO-GANEX PROCESS

The development of an improved EURO-GANEX process is a major goal of the GENIORS project. The EURO-GANEX process is based on the co-extraction of TRU and Ln(III) by a solvent composed of TODGA (Figure 1) and DMDOHEMA (Figure 2) dissolved in kerosene, followed by selective TRU stripping using a solution of SO_3-Ph-BTP (2,6-bis-(5,6-di(sulphophenyl)-1,2,4-triazin-3-yl) pyridine tetrasodium salt)[15] and AHA (acetohydroxamic acid) (Figure 3) in nitric acid.[6-10]

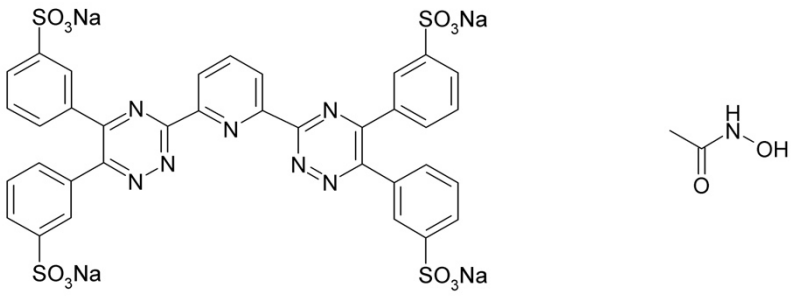

Figure 3. SO_3-Ph-BTP (left) and AHA (right).

Despite the successful hot demonstration of the process, further improvement is envisioned. The complexity of the solvent composition is to be reduced using a single extractant in a kerosene diluent. The TRU stripping solution should contain only complexing agents which are composed of C, H, O, and N, exclusively (the so-called CHON principle).[16] These two issues are being addressed within the GENIORS project.

IMPROVED SOLVENT FORMULATION

The Pu(IV) loading capacity of TODGA solvents is not sufficient for a GANEX application. Hence, the EURO-GANEX solvent additionally contains DMDOHEMA to obtain a sufficient Pu(IV) loading capacity.[6] Another way of improving the loading capacity is increasing the TODGA concentration. This however comes at the price of increased co-extraction of some fission products and more difficult back extraction.

It is known that adding methyl moieties to the DGA backbone substantially lowers distribution ratios for the extraction with TODGA.[17-19] Consequently, *cis*-mTDDGA ((2*R*,2’*S*)-2,2’-oxybis-(*N*,*N*-didecyl-propanamide), Figure 4) was tested as an alternative EURO-GANEX extractant. Indeed, a solvent containing 0.5 mol/L *cis*-mTDDGA in *n*-dodecane has a Pu(IV) loading capacity of > 30 g/L at a nitric acid concentration of 5 mol/L.[20] By replacing *n*-dodecane with Exxsol D80, a Pu(IV) loading capacity of

This project has received funding from the EURATOM research and training programme 2014–2018 under grant agreement No. 755171. The content of this deliverable reflects only the authors’ view. The European Commission is not responsible for any use that may be made of the information it contains.

≥ 50 g/L at a nitric acid concentration of 5 mol/L was achieved (see GENIORS D3.3 and GENIORS HYPAR7-NNL).

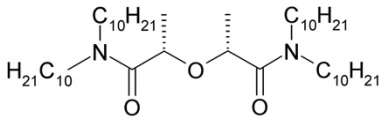

Figure 4. *cis*-mTDDGA.

It is noteworthy that *cis*-mTDDGA (the *RS* diastereomer) is a significantly stronger extracting agent compared to *trans*-mTDDGA (the *RR* diastereomer). This has already been observed for the di-methylated TODGA derivatives.[19]

EXTRACTION OF An, Ln, AND FP BY *cis*-mTDDGA

INITIAL STUDIES

Initial studies were conducted using a solvent containing 0.5 mol/L *cis*-mTDDGA (synthesised by TWENTE as a 3.5:1 mixture of the *cis* and *trans* diasteromers) in Exxsol D80.

NITRIC ACID DEPENDENCY

Distribution ratios for Np, Pu, Am, Cm and Eu as a function of the initial nitric acid concentration are shown in Figure 5. The respective Ln(III) data are shown in Figure 6.

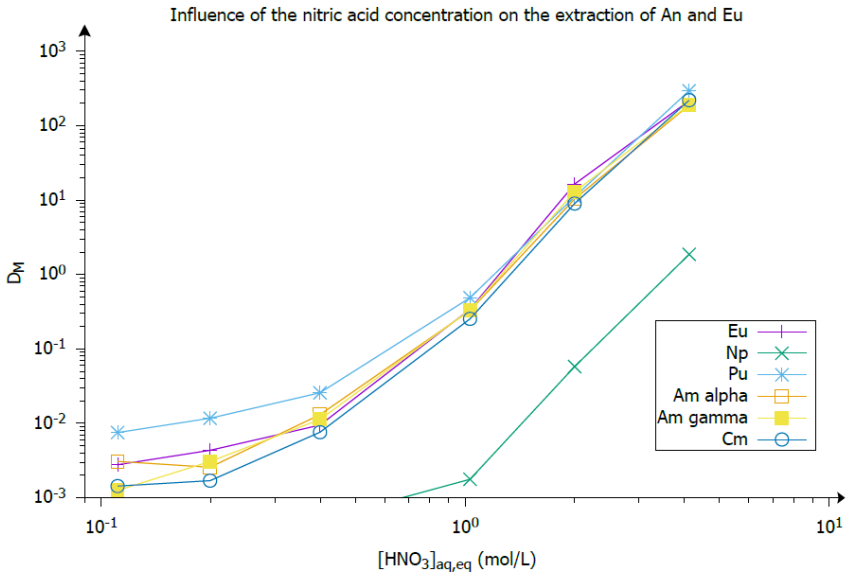

Figure 5: Extraction of An and Eu as a function of the nitric acid concentration. Organic phase, 0.5 mol/L mTDDGA in Exxsol D80, pre-equilibrated. Aqueous phase, each 10^{-5} mol/L Ln + Y + each 1.5 kBq/mL ^{152}Eu, ^{241}Am, ^{244}Cm, ^{239}Pu + 0.74 kBq/mL ^{237}Np in HNO_3. *O/A* = 1, *T* = 25°C, *t* = 60 min, 2500 rpm.

This project has received funding from the EURATOM research and training programme 2014–2018 under grant agreement No. 755171. The content of this deliverable reflects only the authors' view. The European Commission is not responsible for any use that may be made of the information it contains.

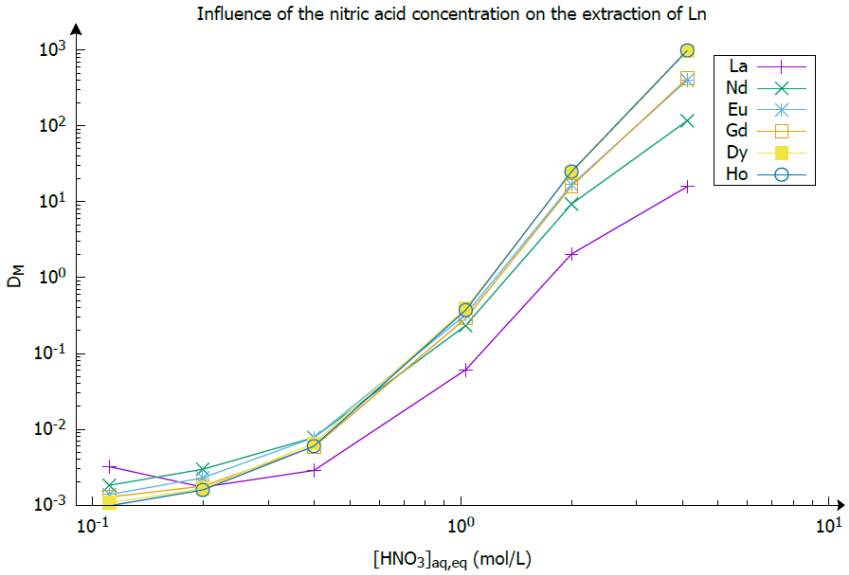

Figure 6. Extraction of Ln as a function of the nitric acid concentration. Experimental conditions see Figure 5.

The distribution ratios of the lanthanides follow a similar trend as the distribution ratios of the actinides (except for Np, as its speciation is known to depend on the nitric acid concentration[21]).

KINETICS

The extraction of actinides is very fast (reaching a plateau after 15 minutes, Figure 7), except for neptunium and plutonium. It is highly probable that the initial oxidation states (+IV for Pu and +V for Np) are not stable under the extraction conditions.

Extraction of the light lanthanides reaches equilibrium after about 15 minutes, see Figure 8. However, heavier lanthanides (e.g. holmium) show a slower extraction.

This project has received funding from the EURATOM research and training programme 2014–2018 under grant agreement No. 755171. The content of this deliverable reflects only the authors' view. The European Commission is not responsible for any use that may be made of the information it contains.

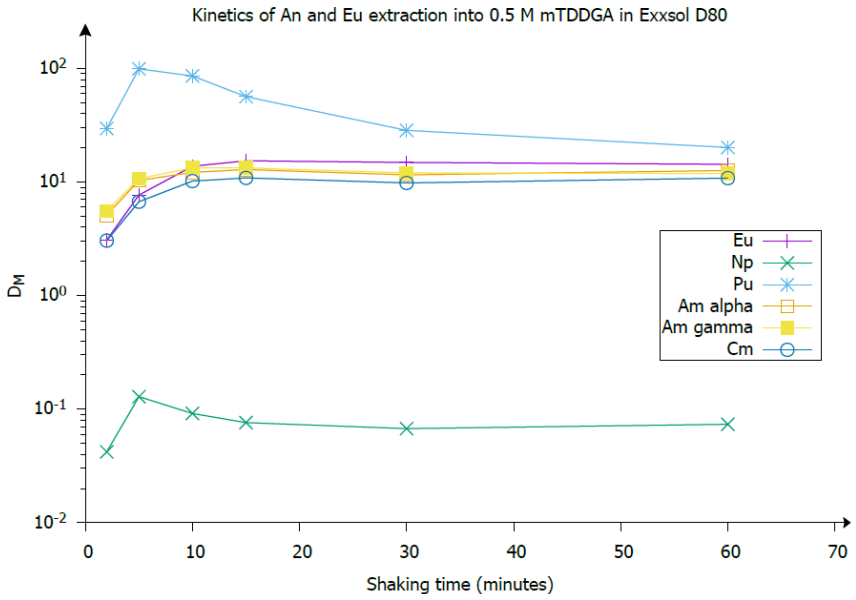

Figure 7: Kinetics of An and Ln extraction. Organic phase, 0.5mol/L mTDDGA in Exxsol D80, pre-equilibrated. Aqueous phase, each 10^{-5} mol/L Ln + Y + each 1.5 kBq/mL ^{152}Eu, ^{241}Am, ^{244}Cm, ^{239}Pu + 0.74 kBq/mL ^{237}Np in 2 mol/L HNO_3. *O/A* = 1, *T* = 25°C, 2500 rpm.

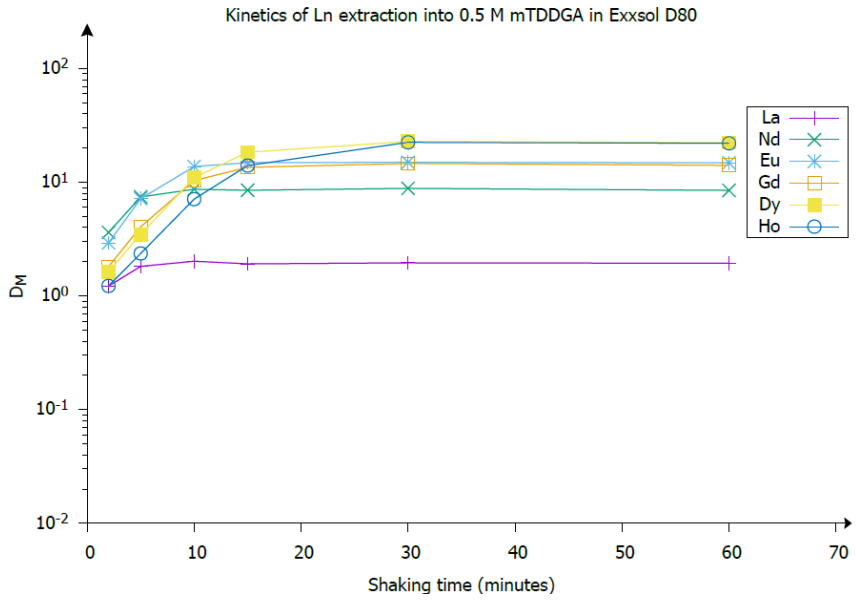

Figure 8: Kinetics of Ln extraction. Experimental conditions see Figure 7.

LIGAND CONCENTRATION DEPENDENCY

Actinide and lanthanide distribution ratios as a function of the extractant concentration are shown in Figure 9 and Figure 10.

This project has received funding from the EURATOM research and training programme 2014–2018 under grant agreement No. 755171. The content of this deliverable reflects only the authors' view. The European Commission is not responsible for any use that may be made of the information it contains.

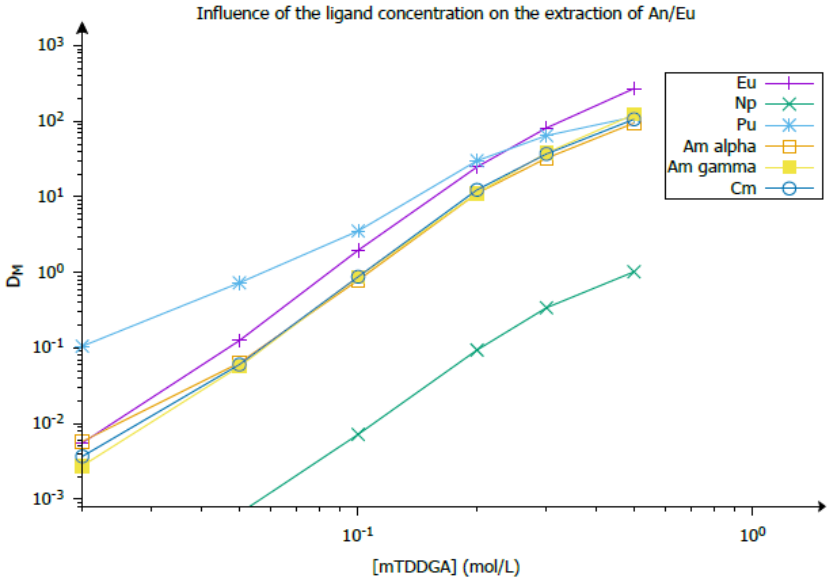

Figure 9: Extraction of An and Ln as a function of the extractant concentration. Organic phase, mTDDGA in Exxsol D80. Aqueous phase, each 10^{-5} mol/L Ln + Y + each 1.5 kBq/mL ^{152}Eu, ^{241}Am, ^{244}Cm, ^{239}Pu + 0.74 kBq/mL ^{237}Np in 4 mol/L HNO_3. *O/A* = 1, *T* = 25°C, *t* = 60 min, 2500 rpm.

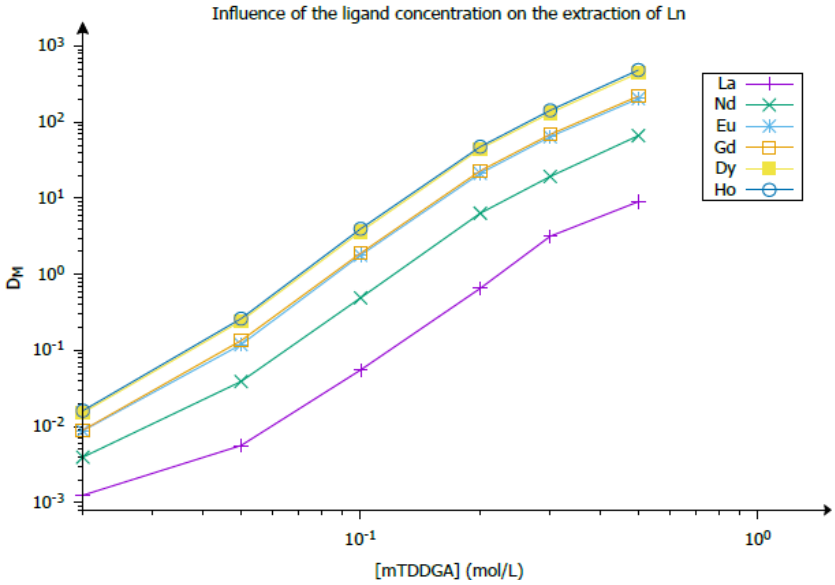

Figure 10: Extraction of An and Ln as a function of the extractant concentration. Experimental conditions see Figure 9.

The slopes for log D vs. log [mTDDGA] are found in Table 1. Since the curve flattens at higher ligand concentrations, the values of the fitting without the highest ligand concentration of 0.5 mol/L are shown in the third column. For neptunium, fitting only starts from 0.1 mol/L mTDDGA. The values for the slopes for Pu and Np extraction deviate, although this could be caused by changes in the oxidation states. For the lanthanides, slopes seem to slightly increase with their mass.

This project has received funding from the EURATOM research and training programme 2014–2018 under grant agreement No. 755171. The content of this deliverable reflects only the authors' view. The European Commission is not responsible for any use that may be made of the information it contains.

Table 1: Slopes of the linear fitting of log(D) as a function of log([ligand]).

Element	Slope	Slope ([mTDDGA] < 0.5 mol/L)
Am (γ)	3.43	3.58
Cm	3.33	3.49
Pu	2.29	2.42
Np	3.11	3.53
Eu	3.45	3.61
La	2.94	2.95
Nd	3.15	3.23
Gd	3.25	3.39
Ho	3.31	3.44

EXTRACTION EXPERIMENTS WITH DIFFERENT DIASTEREOMERIC EXCESSES OF MTDDGA

Three batches of mTDDGA with different diastereomeric excesses were obtained from TWENTE:

- mixture of diastereomers *(cis:trans* = 3.5:1)
- *cis* isomer, *RS*
- *trans* isomer, *SS*

In a first set of experiments 0.1 mol/L of each mTDDGA was tested in Exxsol-D80. A concentration of 0.1 mol/L of each mTDDGA was chosen for two reasons. First, the available amount of the pure diastereomers was low; secondly we wanted to be able to compare the results directly to the results of the extraction of the pure Me_2-TODGA diastereomers.[19]

As known from the scoping study[20] significant extraction was expected only at higher nitric acid concentrations. Therefore, initial nitric acid concentration of 1–6 mol/L were used. Aqueous phase composition is reported in Table 2.

Table 2. Composition of aqueous phases.

Component	Concentration	Component	Concentration	Component	Concentration
Fe	1.8E–05 mol/L	La	1.1E–05 mol/L	Tb	0.9E–05 mol/L
Sr	1.3E–05 mol/L	Ce	1.2E–05 mol/L	Dy	1.2E–05 mol/L
Zr	1.2E–05 mol/L	Pr	1.1E–05 mol/L	Ho	1.2E–05 mol/L
Mo	1.1E–05 mol/L	Nd	1.1E–05 mol/L	Er	0.9E–05 mol/L
Ru	0.9E–05 mol/L	Sm	1.1E–05 mol/L	Tm	0.9E–05 mol/L
Pd	0.7E–05 mol/L	Eu	1.2E–05 mol/L	Yb	1.0E–05 mol/L
Y	1.2E–05 mol/L	Gd	1.1E–05 mol/L	Lu	0.9E–05 mol/L
Tc-99	3.0 MBq/L	Np-237 (V)	2.2 MBq/L	Am-241	3.0 MBq/L
Eu-152	5.6 MBq/L	Pu-239	6.6 MBq/L	Cm-244	3.0 MBq/L
HNO_3	1–6 mol/L				

This project has received funding from the EURATOM research and training programme 2014–2018 under grant agreement No. 755171. The content of this deliverable reflects only the authors' view. The European Commission is not responsible for any use that may be made of the information it contains.

The phases were contacted for 30 minutes, which is expected to be sufficient to attain equilibrium. Figure 11 shows the distribution ratios of Np-237, Pu-239, and Am-241 as a function of the nitric acid concentration. For Am-241 a clear difference in the extraction is observed with the cis (*RS*) isomer extracting the best. The trans isomer (*SS*) extracts significantly less and for the mixture distribution ratios in between are measured (as expected). Pu extraction however differs, as the difference in extraction between the different diastereomers is rather small. The Np extraction is hard to get a clear picture of, as the distribution ratios are generally quite low, and Np is only extracted at the highest HNO_3 concentrations.

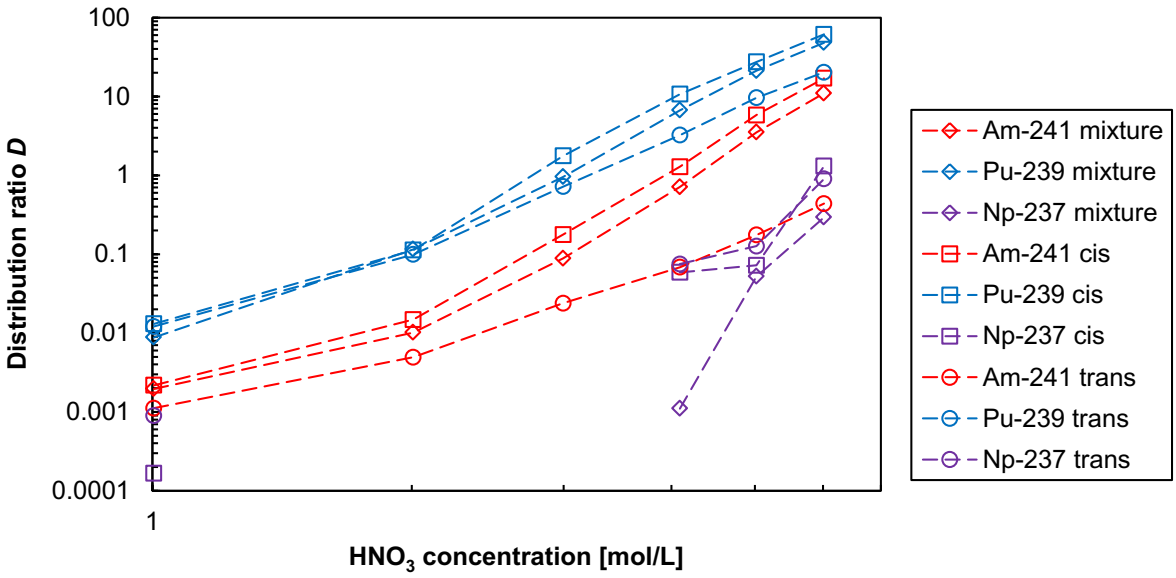

Figure 11. Extraction of Np-237, Pu-239, and Am-241 as a function of the nitric acid concentration. Organic phase, 0.1 mol/L mTDDGA (different diastereomers) in Exxsol-D80. see Table 2. *O/A* = 1, *T* = 22°C, *t* = 30 min.

Figure 12 shows the distribution ratios of Am-241 and Cm-244 as a function of the nitric acid concentration. Here, the same principal trend is observed, with the cis (*RS*) isomer extracting the best, the trans isomer (*SS*) extracting significantly less and intermediate distribution ratios for the mixture. Interestingly, an inversion of selectivity is observed, similar to the same phenomenon that had been observed with the different diastereomers of Me_2-TODGA.[19] The cis (*RS*) isomer and the mixture show a preference for Cm over Am extraction, while the trans isomer (*SS*) shows the opposite selectivity.

This project has received funding from the EURATOM research and training programme 2014–2018 under grant agreement No. 755171. The content of this deliverable reflects only the authors' view. The European Commission is not responsible for any use that may be made of the information it contains.

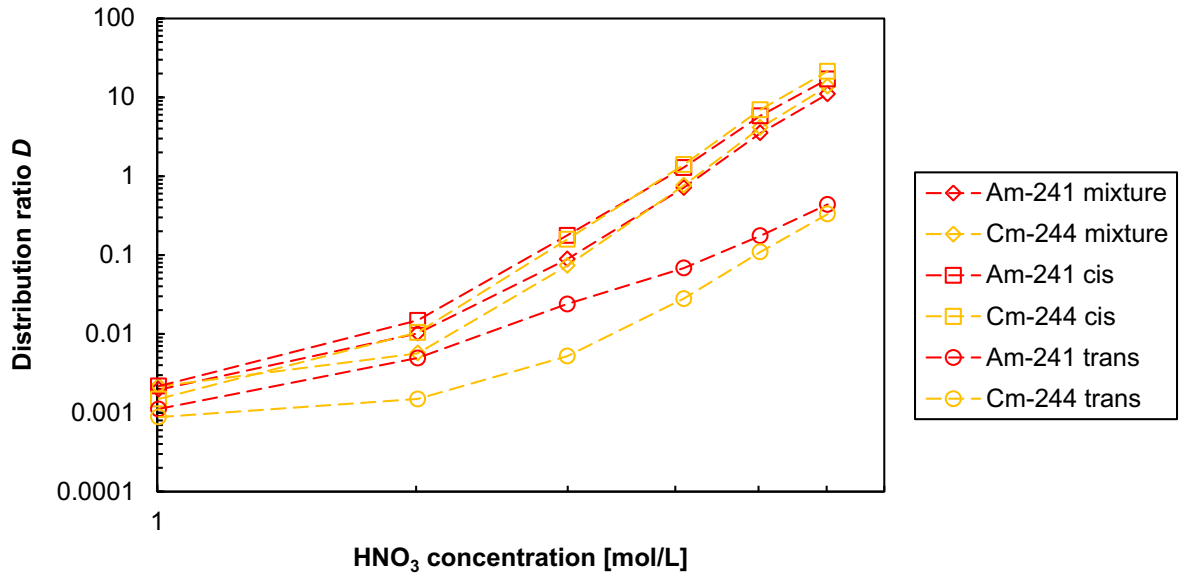

Figure 12. Extraction of Am and Cm as a function of the nitric acid concentration. Experimental conditions see Figure 11.

Figure 13 shows an overview of distribution ratios of all metal ions for different diastereomers of mTDDGA and nitric acid concentrations. Most metal ions show the same trends in nitric acid concentration (increasing distribution ratios with increasing nitric acid concentration) and order of diastereomers (cis > mixture > trans). The Ln extraction pattern shows a maximum for the extraction of Er, which is comparable to Me_2-TODGA.[19]

Ru and Sr distribution ratios were low under all conditions.

Tc extraction doesn't follow the trend in nitric acid concentration, which could be explained by its extraction as anion. It follows the order of diastereomers (cis > mixture > trans).

Fe, Pd, and Mo extraction don't follow the trends. Their distribution ratios are nearly independent of the HNO_3 concentration, and they follow a different order of diastereomers: trans > cis > mixture. Even though it could be possible that the trans isomer extracts these metal ions better, the order of diastereomers doesn't make much sense, as the mixture of diastereomers should show an intermediate behaviour in any case. Therefore, the Fe, Pd, and Mo extraction is currently not understood and further experiments are needed to understand their behaviour.

This project has received funding from the EURATOM research and training programme 2014–2018 under grant agreement No. 755171. The content of this deliverable reflects only the authors' view. The European Commission is not responsible for any use that may be made of the information it contains.

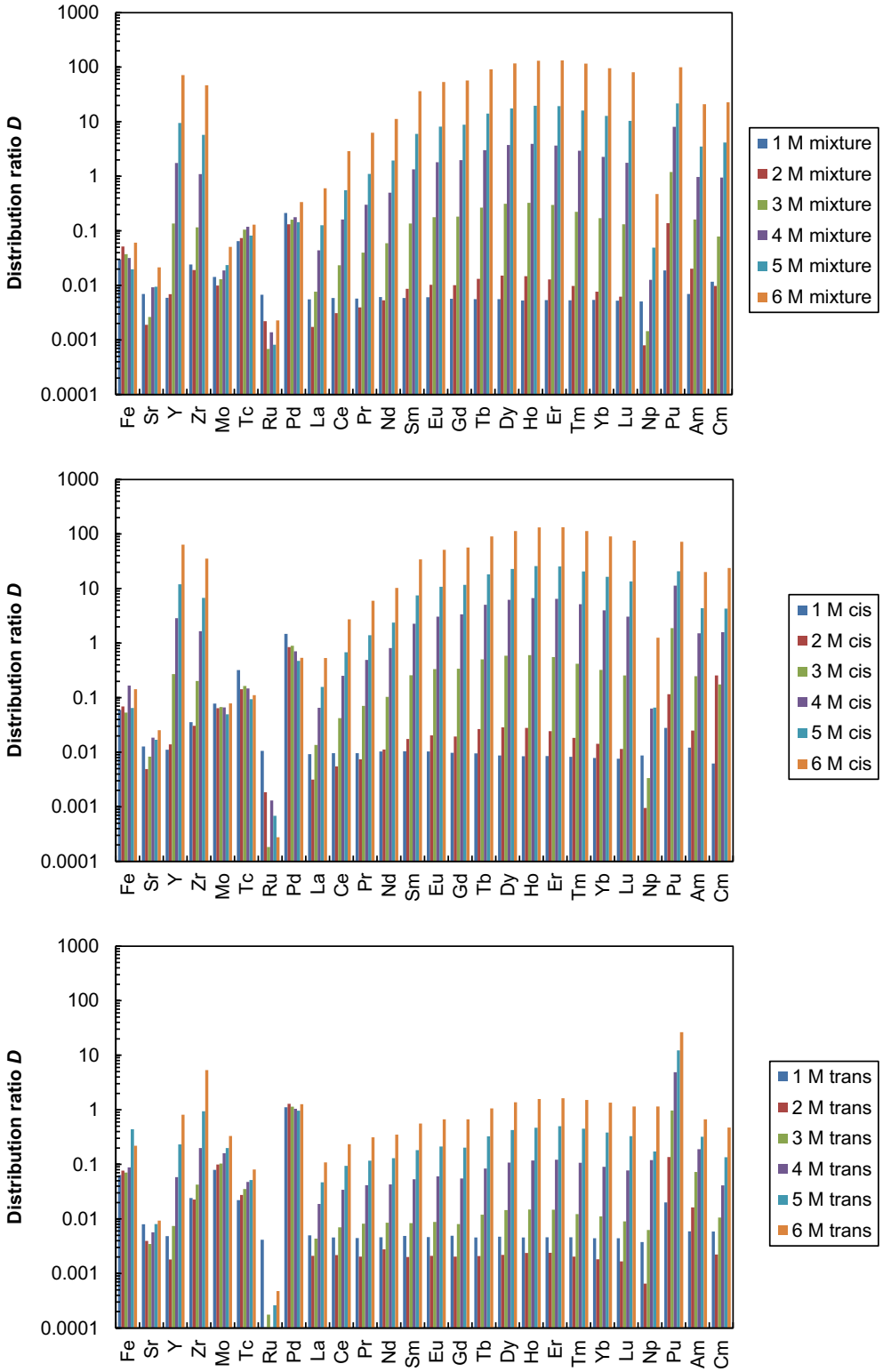

Figure 13. Extraction of all metal ions as a function of the nitric acid concentration. Experimental conditions see Figure 11.

This project has received funding from the EURATOM research and training programme 2014–2018 under grant agreement No. 755171. The content of this deliverable reflects only the authors' view. The European Commission is not responsible for any use that may be made of the information it contains.

DETAILED STUDIES WITH *cis*-mTDDGA

For more detailed studies, two batches of *cis*-mTDDGA were used: one small batch obtained from TWENTE University (Enschede, The Netherlands) and a larger batch obtained from Oak Ridge National Laboratory (Oak Ridge, TN, USA). The diastereomeric excess (*de*) of the Oak Ridge batch is approx. 30:1 *cis* over *trans* (93.5% *de*).

Figure 14 and Figure 15 show the distribution ratios for actinides and all fission and corrosion products tested.

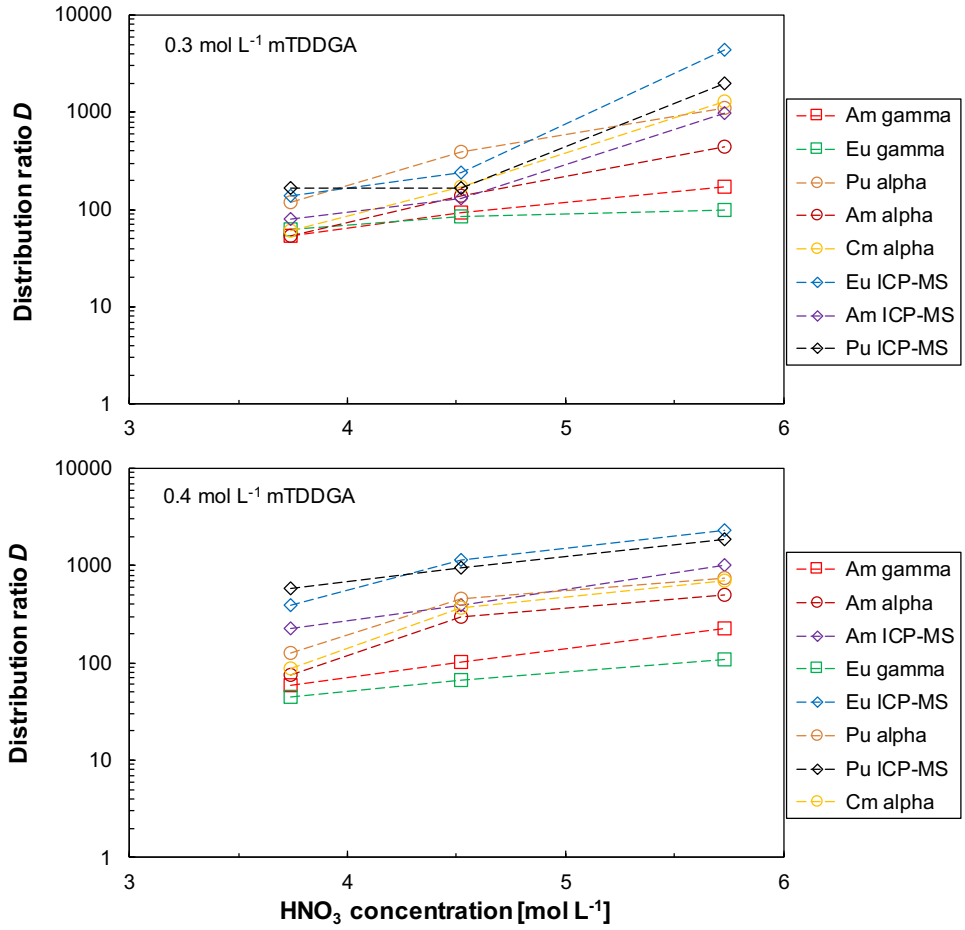

Figure 14. Distribution ratios *D* as a function of the HNO_3 concentration for 0.3 mol/L (top) and 0.4 mol/L (bottom) *cis*-mTDDGA (Twente). Organic phase, *cis*-mTDDGA in *n*-dodecane. Aqueous phase, 10^{-5} mol/L Ln and FP in HNO_3, spiked with ^{152}Eu, ^{239}Pu, ^{241}Am, and ^{244}Cm. 22°C, 2,220 rpm, 60 min.

Am^{3+}, Cm^{3+} and Pu^{4+} were well extracted with high distribution ratios. The variation in the distribution ratios comparing different analytical techniques was rather high, presumably due to the high *D* values and related experimental uncertainties. The maximum in extractability within the Ln series (+Y) was observed for Ho, which is the same as observed for *cis*-Me_2-TODGA.[19] The least extractable lanthanide ion is La^{3+}. A co-extraction of Sr, Zr, and Pd was observed without showing a distinct nitric acid

This project has received funding from the EURATOM research and training programme 2014–2018 under grant agreement No. 755171. The content of this deliverable reflects only the authors' view. The European Commission is not responsible for any use that may be made of the information it contains.

dependency. It is expected that the co-extraction of Zr and Pd can be suppressed using CDTA in the extraction stage.[23] Fe and Mo distribution ratios were < 1, and Ru distribution ratios < 0.01. These metal ions are not expected to be problematic.

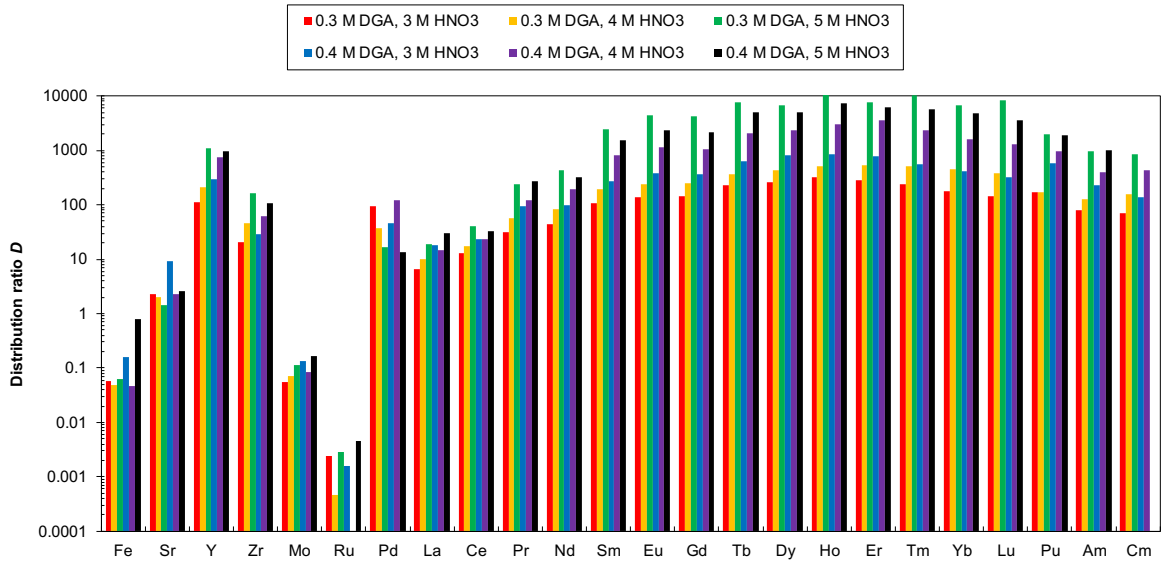

Figure 15. Distribution ratios *D* of actinides, lanthanides and fission products as a function of *cis*-mTDDGA and HNO_3 concentrations (ICP-MS measurement). Experimental details see Figure 14.

Figure 16 shows the Am distribution ratios *D* as a function of the HNO_3 concentration for the extraction with different concentrations and batches of *cis*-mTDDGA. The shaking time was different for different experimental series between 15–60 min, but 15 min is expected sufficient to reach the equilibrium. Therefore, all data are equilibrium data. The results show good comparison between the different batches of *cis*-mTDDGA, although the number of data points measured under identical conditions is limited. The new *cis*-mTDDGA batch obtained from Oak Ridge showed very comparable extraction results in comparison to the batch obtained from TWENTE. Data scattered more for Eu and Pu in the directly comparable high HNO_3 concentration range, due to the high *D* values and associated uncertainties.

This project has received funding from the EURATOM research and training programme 2014–2018 under grant agreement No. 755171. The content of this deliverable reflects only the authors' view. The European Commission is not responsible for any use that may be made of the information it contains.

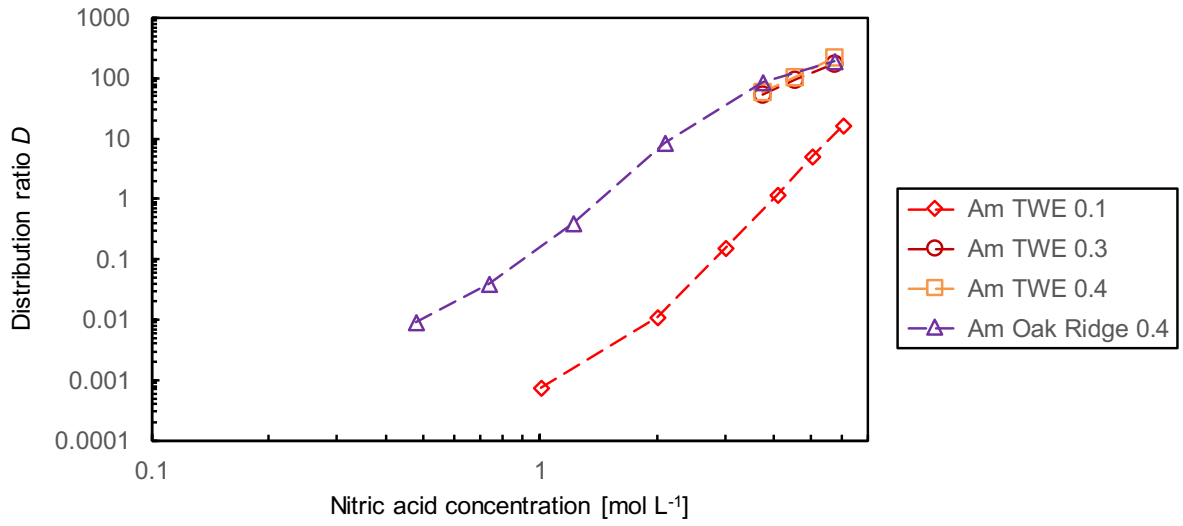

Figure 16. Extraction of Am batches of *cis*-mTDDGA. Organic phase, *cis*-mTDDGA (TWENTE or Oak Ridge) in *n*-dodecane. Aqueous phase, 10^{-5} mol/L Ln and FP in HNO_3, spiked with ^{152}Eu, ^{239}Pu, ^{241}Am, and ^{244}Cm. 22°C, 2,220 rpm, 15–60 min.

Figure 17 shows increasing distribution ratios as a function of the HNO_3 concentration for 0.4 mol/L *cis*-mTDDGA (Oak Ridge), and Figure 18 shows an overview of all metal ions. Interestingly, the maximum in extractability within the Ln series (+Y) is shifted to Eu for the Oak Ridge *cis*-mTDDGA batch, while the TWENTE batch showed a maximum at Ho. The reason for that shift is unclear. The least extractable of the light lanthanides is still La. A slight co-extraction of Sr and stronger co-extraction of Zr was observed showing increasing *D* values with increasing HNO_3 concentrations. Pd showed *D* values of 2–7 without showing a distinct nitric acid dependency. Fe and Mo distribution ratios were < 1, and Ru distribution ratios even < 0.01. These metal ions hence are expected not be an issue.

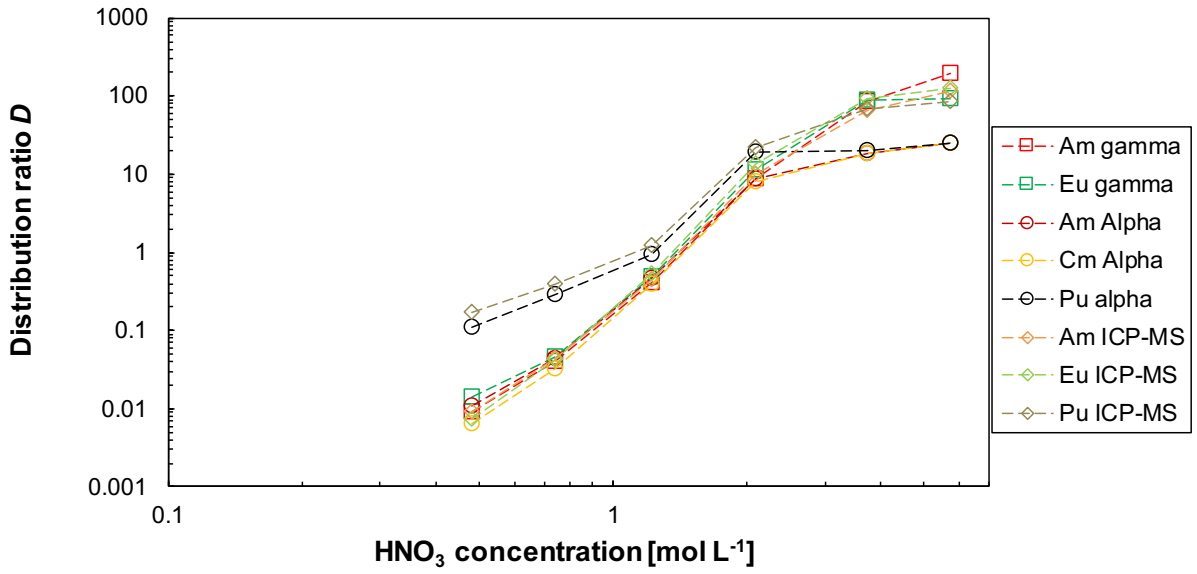

Figure 17. Extraction of An and Eu. Organic phase, 0.4 mol/L *cis*-mTDDGA (Oak Ridge) in *n*-dodecane. Aqueous phase, 10^{-5} mol/L Ln and FP in HNO_3, spiked with ^{152}Eu, ^{239}Pu, ^{241}Am, and ^{244}Cm. 22°C, 2,220 rpm, 15 min.

This project has received funding from the EURATOM research and training programme 2014–2018 under grant agreement No. 755171. The content of this deliverable reflects only the authors' view. The European Commission is not responsible for any use that may be made of the information it contains.

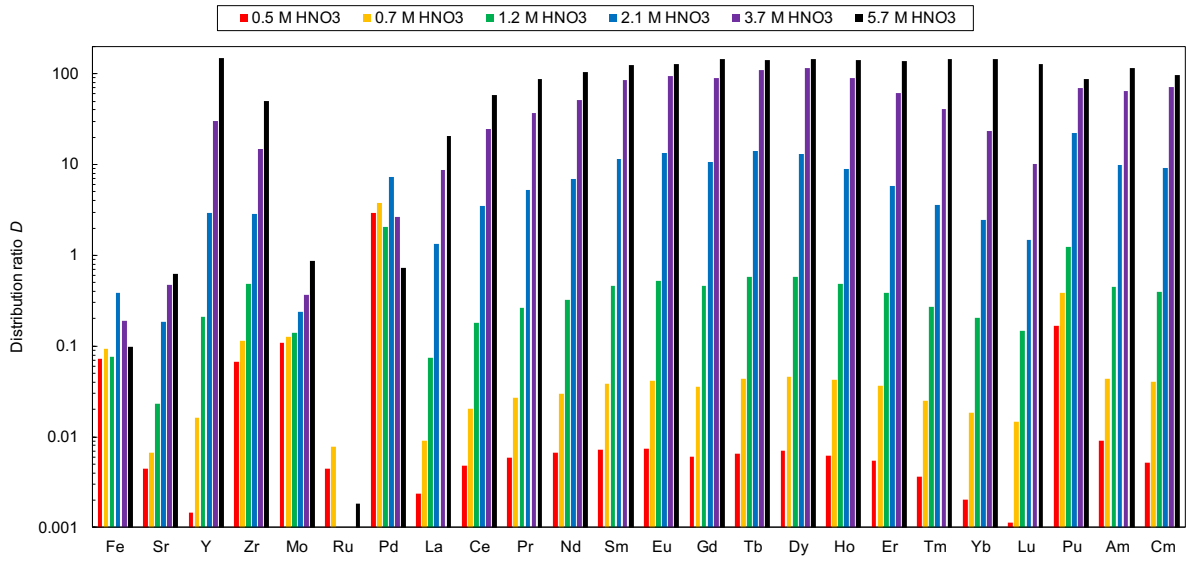

Figure 18. Extraction of all metal ions studied Experimental conditions see Figure 17.

EXTRACTION OF HNO_3 BY *cis*-mTDDGA

Initial nitric acid tests were performed with *trans*-mTDDGA due to limited availability of the *cis* diastereomer. The idea was to run a few additional tests with *cis*-mTDDGA and hopefully find a simple relation between the two.

Results are shown in Figure 19.

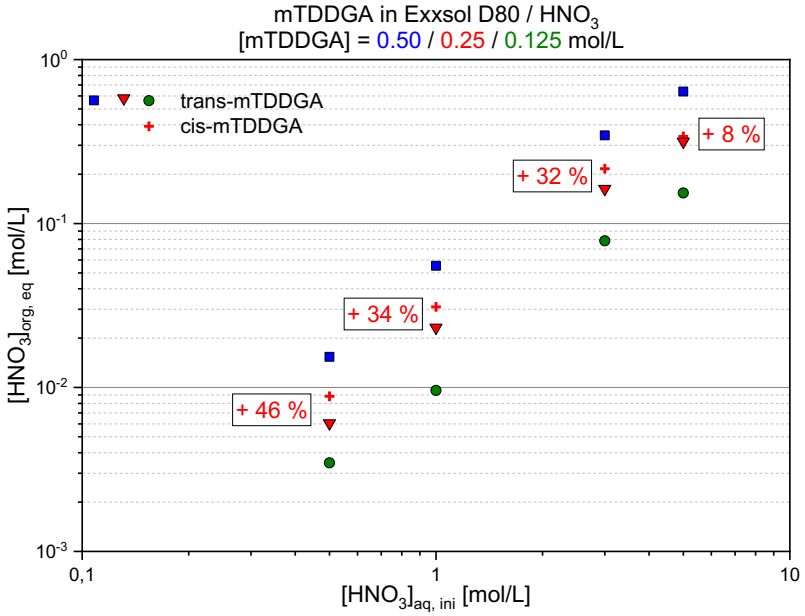

Figure 19. Nitric acid extraction into *cis/trans*-mTDDGA dissolved in Exxsol D80. *A/O* = 1, *t* = 30 min, *T* = 20 °C.

This project has received funding from the EURATOM research and training programme 2014–2018 under grant agreement No. 755171. The content of this deliverable reflects only the authors' view. The European Commission is not responsible for any use that may be made of the information it contains.

Two observations were made:

1. For an initial nitric acid concentration of 5 mol/L, the organic nitric acid concentration exceeds the extractant concentration. This is explained by the formation of adducts, $(HNO_3)_n$DGA, with $n \geq 2$. Such adducts are found for many extractants, e. g. TODGA,[11] DMDOHEMA,[14] *n*-Pr-BTP,[24] PTEH (see below).
2. *cis*-mTDDGA extracts significantly more nitric acid than does *trans*-mTDDGA. There is no simple correlation such as a constant factor. (+ 46% at $[HNO_3]_{aq,ini}$ = 0.5 mol/L, steadily decreasing to + 8% at $[HNO_3]_{aq,ini}$ = 5 mol/L).

Figure 20 shows the extraction of nitric acid by 0.4 mol/L *cis*-mTDDGA (Oak Ridge). The data is roughly comparable with that shown in Figure 19, although not directly comparable due to differences in the experimental conditions. The HNO_3 distribution ratio is approx. 0.1.

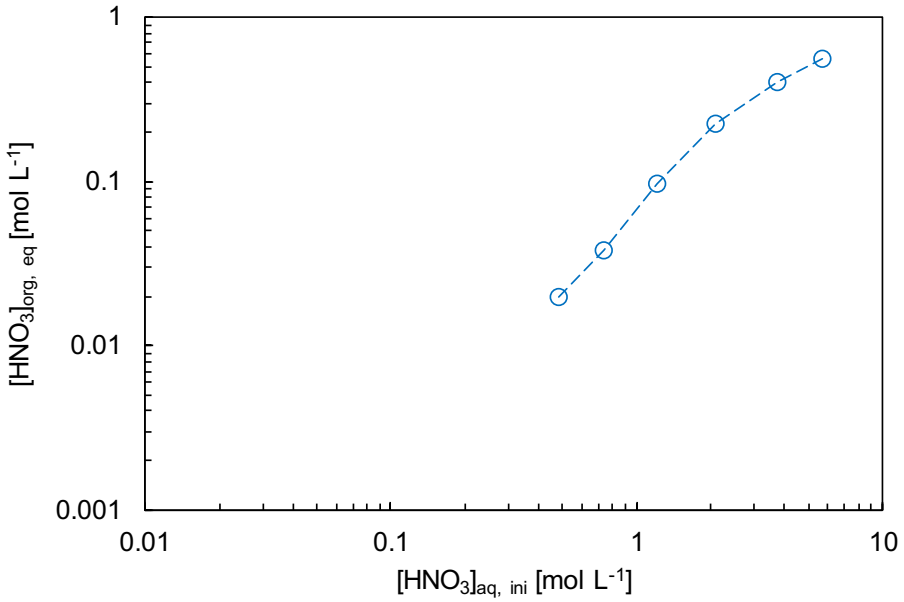

Figure 20. Organic nitric acid concentration as a function of the initial aqueous nitric acid concentration for the extraction with 0.4 mol/L *cis*-mTDDGA (Oak Ridge). Experimental details see Figure 17.

IMPROVED TRU STRIPPING SOLUTION FORMULATION

The sulphur content of SO_3-Ph-BTP (the complexing agent used to selectively strip Am(III) and Cm(III) from the loaded EURO-GANEX solvent) is prohibitive to an application on the industry scale. Consequently, PTD (2,6-bis[1-(propanol)-1,2,3-triazol-4-yl]pyridine, Figure 21)[25-27] was assessed for this task. Initial experiments were conducted using both the EURO-GANEX solvent and the *cis*-mTDDGA solvent.

This project has received funding from the EURATOM research and training programme 2014–2018 under grant agreement No. 755171. The content of this deliverable reflects only the authors' view. The European Commission is not responsible for any use that may be made of the information it contains.

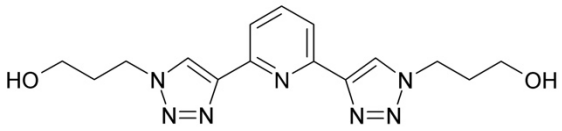

Figure 21. PTD.

USING PTD TO STRIP TRU FROM THE EURO-GANEX SOLVENT

PTD was tested as an alternative for the non-CHON SO_3-Ph-BTP to selectively back-extract actinides from a loaded EURO-GANEX organic phase.

Organic phases were 0.2 mol/L TODGA and 0.5 mol/L DMDOHEMA in Exxsol D80. Aqueous phases contained 0.04–0.12 mol/L PTD in 0.05–1 mol/L nitric acid. Distribution ratios for Y(III), all Ln(III) (except Pm(III)), Pu(IV) and Am(III) at a PTD concentration of 0.08 mol/L are shown in Figure 22. Distribution ratios for La(III), Ho(III), Pu(IV) and Am(III) at different PTD concentrations are given in Figure 23.

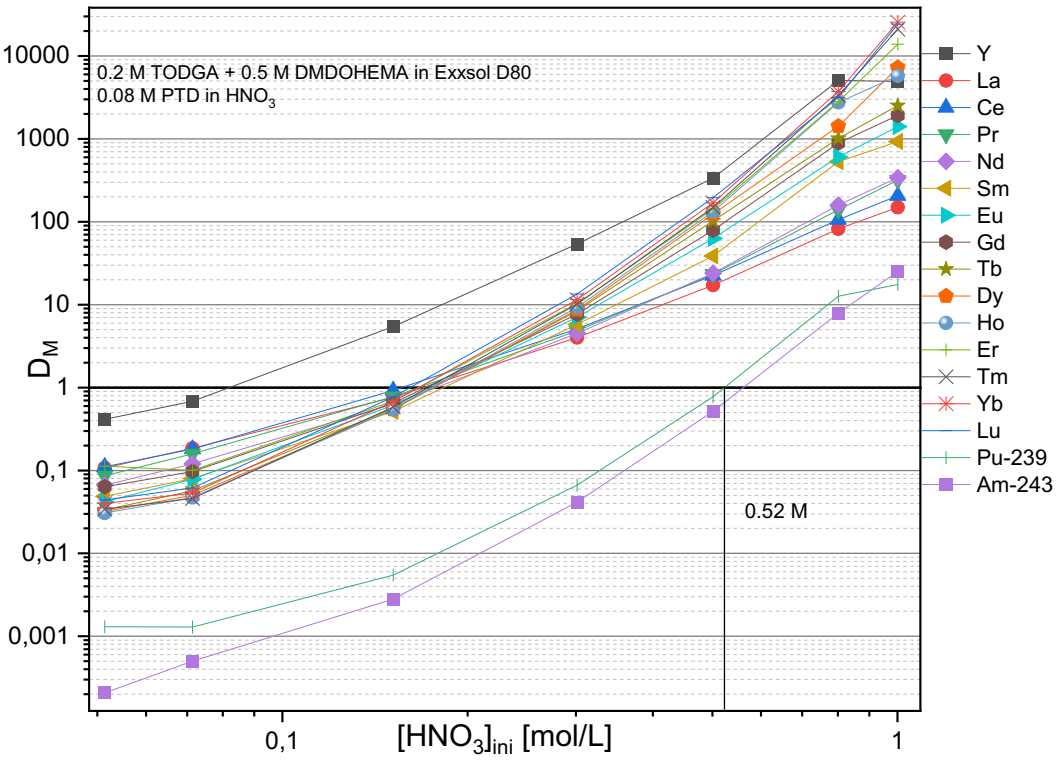

Figure 22. Distribution ratios for Am(III), Pu(IV), Y(III), Ln(III) in the TODGA/DMDOHEMA/PTD system as a function of the nitric acid concentration. Organic phase, 0.2 mol/L TODGA + 0.5 mol/L DMDOHEMA in Exxsol D80. Aqueous phase, 0.08 mol/L PTD in 0.05–1 mol/L HNO_3. *A/O* = 1, *T* = 293 K; *t* = 30 min.

This project has received funding from the EURATOM research and training programme 2014–2018 under grant agreement No. 755171. The content of this deliverable reflects only the authors' view. The European Commission is not responsible for any use that may be made of the information it contains.

Pu(IV) and Am(III) show distribution ratios below one for [HNO_3] > 0.41 – 0.6 mol/L with Pu(IV) having slightly greater distribution ratios than Am(III).

Y(III) is extracted for [HNO_3] > 0.06–0.09 mol/L (with increasing PTD concentration). Ln(III) are extracted for [HNO_3] > 0.12–0.2 mol/L (with increasing PTD concentration). Light lanthanides (La, Ce) show the lowest distribution ratios at high [HNO_3], however, at low [HNO_3] the heavy lanthanides (Ho–Lu, with Ho being the lowest) are extracted the least.

With a PTD concentration of 0.08 mol/L, Pu(IV) and Am(III) are separated from Ln(III) with a An/Ln selectivity of 20–100 in a nitric acid concentration range of 0.2–0.5 mol/L.

PTD shows promise as a CHON stripping agent for the EURO-GANEX process for selectively stripping actinides from a loaded TODGA/DMDOHEMA solvent. and potentially replace SO_3-Ph-BTP.Further studies are required to evaluate whether PTD can replace SO_3-Ph-BTP in a EURO-GANEX process.

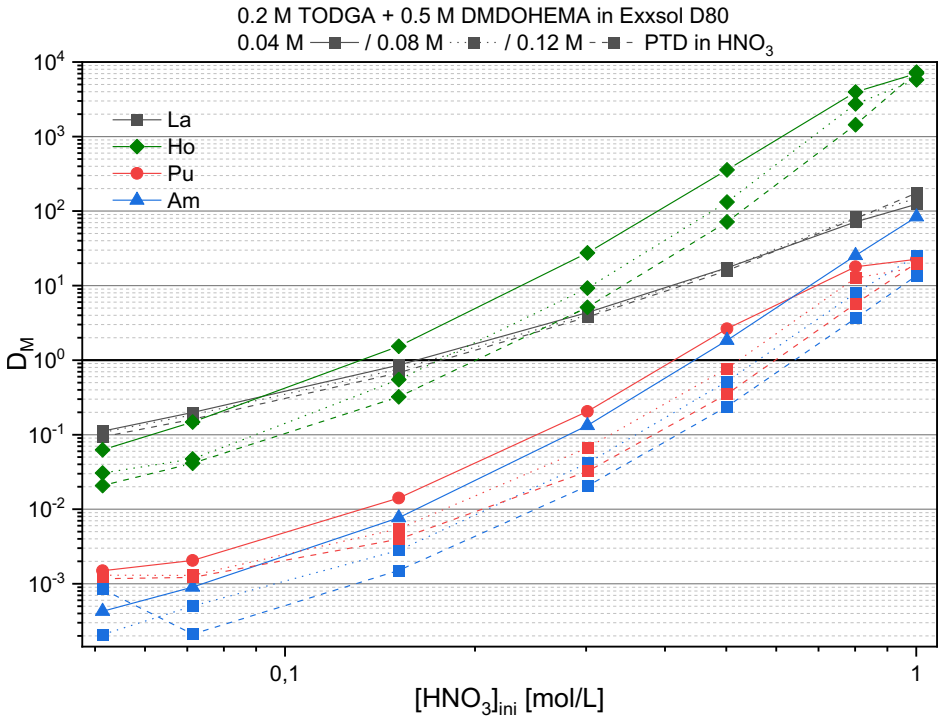

Figure 23. Distribution ratios for Pu(IV), Am(III), La(III), Ho(III) in the TODGA/DMDOHEMA/PTD system as a function of the nitric acid and PTD concentrations. Organic phase, 0.2 mol/L TODGA + 0.5 mol/L DMDOHEMA in Exxsol D80. Aqueous phase, 0.04–0.12 mol/L PTD in 0.05–1 mol/L HNO_3. *A/O* = 1, *T* = 293 K; *t* = 30 min.

USING PTD TO STRIP TRU FROM A *cis*-mTDDGA SOLVENT

In a first series of extraction experiments a fixed PTD concentration of 0.04 mol/L was chosen and the extraction with 0.4 mol/L *cis*-mTDDGA was tested as a function of the HNO_3 concentration. Figure 24 shows the Am and Eu distribution ratios in comparison with a series of extractions without PTD addition. The *D* values increased with increasing HNO_3 concentration. The Am/Eu selectivity was not

This project has received funding from the EURATOM research and training programme 2014–2018 under grant agreement No. 755171. The content of this deliverable reflects only the authors' view. The European Commission is not responsible for any use that may be made of the information it contains.

much increased by the addition of PTD. In the range of 0.5–1.2 mol/L HNO_3 slightly lower *D* values were measured for the experiments with added PTD compared to the one without PTD addition. The separation factor $SF_{Eu/Am}$ did not exceed a value of 5.

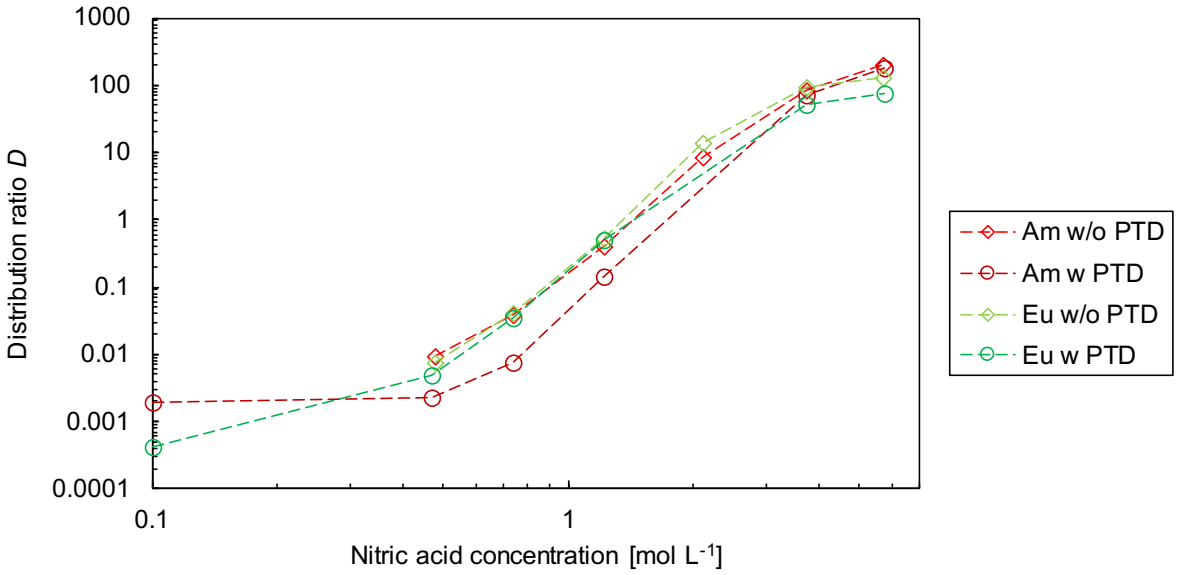

Figure 24. Distribution ratios *D* as a function of the nitric acid concentration for the extraction with 0.4 mol/L *cis*-mTDDGA (Oak Ridge) with and without addition of 0.04 mol/L PTD. Organic phase, 0.4 mol/L *cis*-mTDDGA (Oak Ridge) in *n*-dodecane. Aqueous phase, 10^{-5} mol/L Ln and FP in HNO_3, with and without addition of 0.04 mol/L PTD, spiked with 152Eu, 239Pu, ^{241}Am, and ^{244}Cm. 22°C, 2,220 rpm, 15 min.

Figure 25 shows increasing distribution ratios of Am, Eu, Cm, and Pu as a function of the HNO_3 concentration for 0.4 mol/L *cis*-mTDDGA (Oak Ridge) with addition of 0.04 mol/L PTD, and Figure 26 shows an overview of all metal ions. The maximum in extractability within the Ln series (+Y) varies much for the different nitric acid concentrations, and no clear trend can be recognized. The least extractable of the light lanthanides (La–Gd) is still La. Increasing co-extraction of Sr, Zr and Mo was observed with increasing HNO_3 concentrations. Pd and Fe showed *D* values of approx. 0.1 without showing a distinct nitric acid dependency. Ru distribution ratios are below 0.01. Figure 27 shows the extraction of nitric acid by 0.4 mol/L *cis*-mTDDGA (Oak Ridge) with addition of 0.04 mol/L PTD. The nitric acid extraction is practically identical to the one without addition of PTD shown in Figure 20.

This project has received funding from the EURATOM research and training programme 2014–2018 under grant agreement No. 755171. The content of this deliverable reflects only the authors' view. The European Commission is not responsible for any use that may be made of the information it contains.

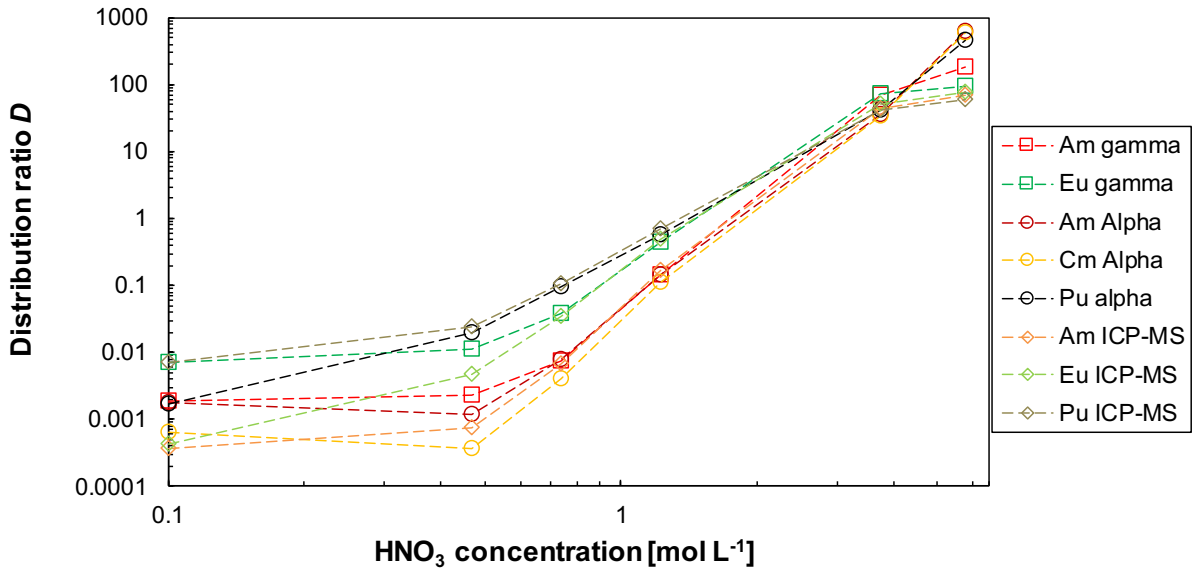

Figure 25. Distribution ratios *D* as a function of the nitric acid concentration for the extraction with 0.4 mol/L *cis*-mTDDGA (Oak Ridge) with addition of 0.04 mol/L PTD. Organic phase, 0.4 mol/L *cis*-mTDDGA (Oak Ridge) in *n*-dodecane. Aqueous phase, 10^{-5} mol/L Ln and FP in HNO_3, 0.04 mol/L PTD, spiked with ^{152}Eu, ^{239}Pu, ^{241}Am, and ^{244}Cm. 22°C, 2,220 rpm, 15 min.

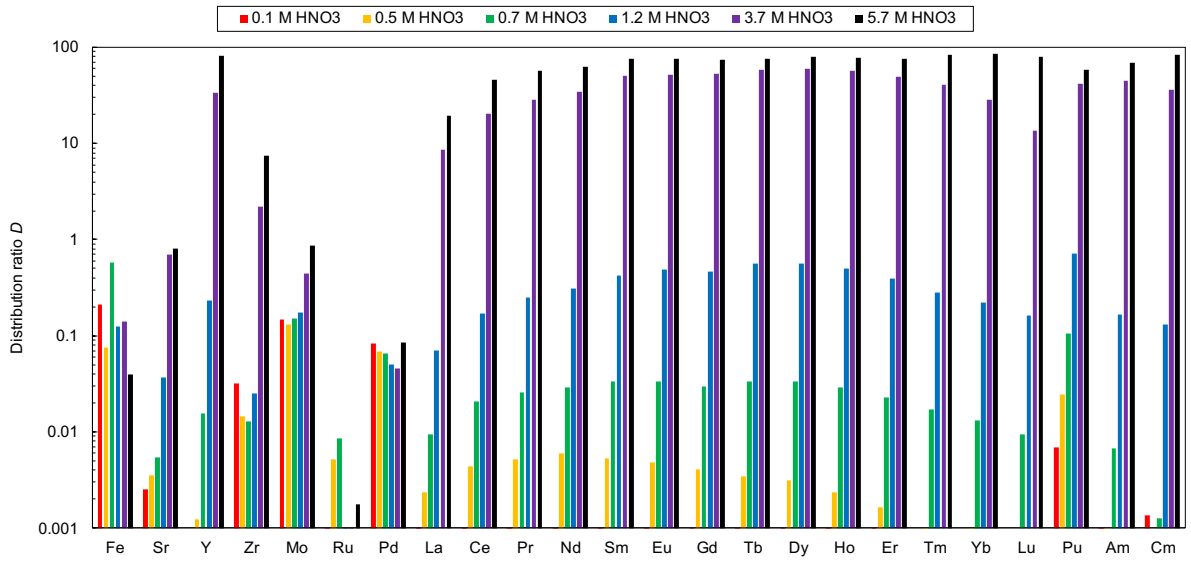

Figure 26. Distribution ratios D as a function of the nitric acid concentration for the extraction with 0.4 mol/L *cis*-mTDDGA (Oak Ridge) with addition of 0.04 mol/L PTD. Experimental details see Figure 25.

This project has received funding from the EURATOM research and training programme 2014–2018 under grant agreement No. 755171. The content of this deliverable reflects only the authors' view. The European Commission is not responsible for any use that may be made of the information it contains.

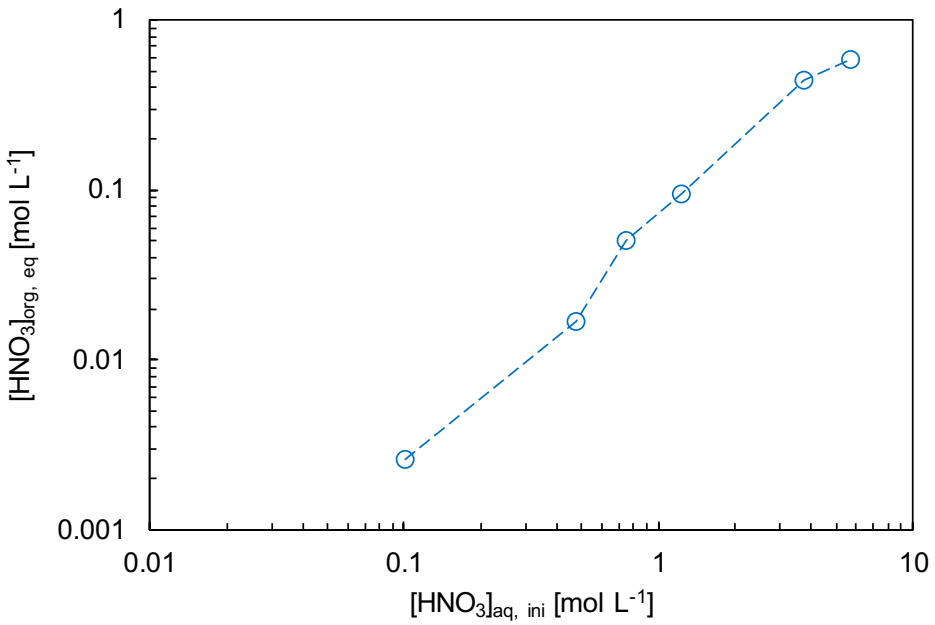

Figure 27. Organic equilibrium nitric acid concentration as a function of the initial aqueous nitric acid concentration for the extraction with 0.4 mol/ cis-mTDDGA (Oak Ridge) with addition of 0.04 mol/L PTD. Experimental details see Figure 25.

In the next series, the PTD concentration was varied in the range of 0–0.4 mol/L PTD at 2.1 mol/L HNO_3 and 0.4 mol/L *cis*-mTDDGA. The results in Figure 28 and Figure 29 show decreasing distribution ratios for all metal ions with increasing PTD concentration. The trivalent actinides Am and Cm were affected the most, resulting in increasing $SF_{Eu/Am}$ (≤ 23) and $SF_{Pu/Am}$ (≤ 14) separation factors. The Am/Cm selectivity remained unchanged with $SF_{Am/Cm} \approx 1.5$. Figure 29 shows the *D* values for Am and the light lanthanides (La–Gd) as a function of the PTD concentration. The separation of Am from the lanthanides is governed by the least extractable La. Am *D* values fall below the La *D* values at PTD concentrations > 0.2 mol/L, but with a low $SF_{La/Am}$ of 1.4. The best separation, $SF_{La/Am} = 4.8$, was achieved at 0.4 mol/L PTD, but with a La *D* value of 0.56.

Figure 30 shows the distribution ratios for all investigated metal ions. Again, the maximum in extractability within the Ln series (+Y) is shifted to Eu, also for the experiment with addition of PTD. Zr and Pd distribution ratios also decrease strongly with increasing PTD concentration, while little to no effect was observed for Fe, Sr, and Mo. Ru distribution ratios were generally very low.

HNO_3 extraction was relatively constant with *D* values of approx. 0.1, but an overall decreasing HNO_3 concentration was observed. This is probably caused by partial protonation of PTD, consuming approx. half the amount (in mol) HNO_3 per mol PTD.

The same PTD concentration range (0–0.4 mol/L) was also tested at 3.7 mol/L HNO_3 and 0.4 mol/L *cis*-mTDDGA. Figure 31 shows that distribution ratios were generally higher compared to the extraction from 2.1 mol/L HNO_3, as expected for the higher nitric acid concentration. At any PTD concentration,

This project has received funding from the EURATOM research and training programme 2014–2018 under grant agreement No. 755171. The content of this deliverable reflects only the authors' view. The European Commission is not responsible for any use that may be made of the information it contains.

Am *D* values were ≥ 10 and no separation from La was achieved. The use of > 2 mol/L HNO_3 is therefore not usable for the selective Am stripping.

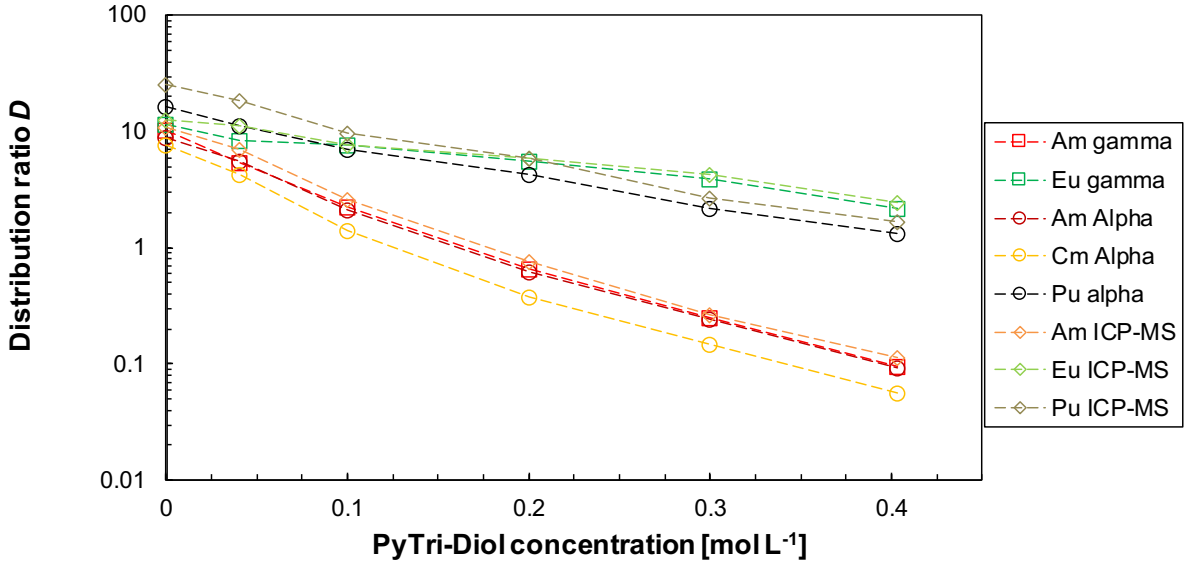

Figure 28. Distribution ratios *D* as a function of the PTD concentration for extraction with 0.4 mol/L *cis*-mTDDGA (Oak Ridge) from 2.1 mol/L HNO_3. Organic phase, 0.4 mol/L *cis*-mTDDGA (Oak Ridge) in *n*-dodecane. Aqueous phase, 10^{-5} mol/L Ln and FP in 2.1 mol/L HNO_3, spiked with ^{152}Eu, ^{239}Pu, ^{241}Am, and ^{244}Cm. 22°C, 2,220 rpm, 15 min.

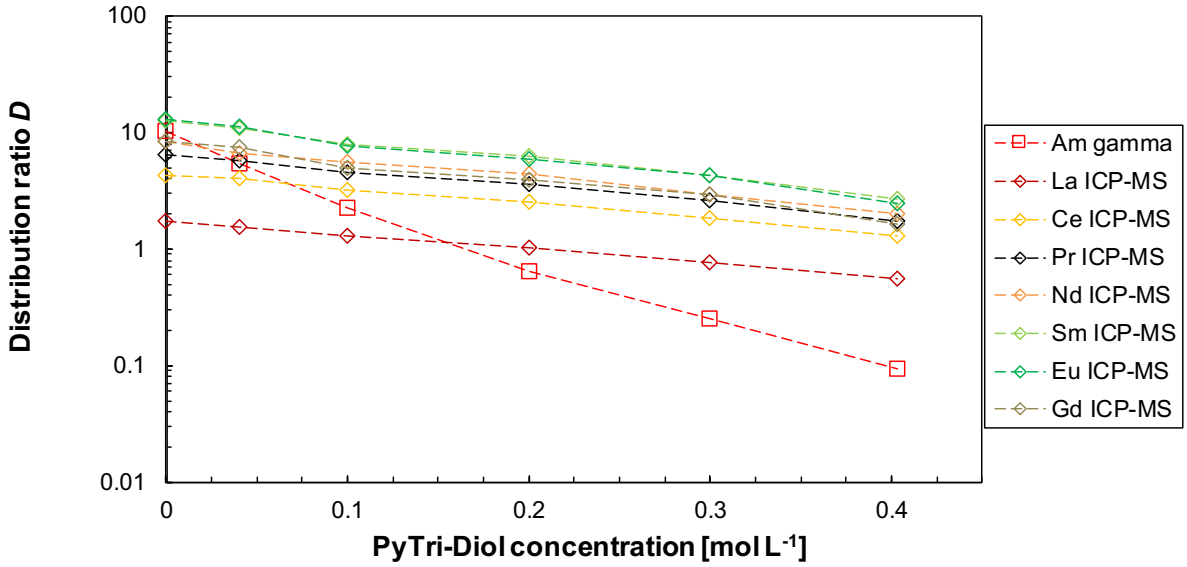

Figure 29. Distribution ratios *D* as a function of the PTD concentration for extraction with 0.4 mol/L *cis*-mTDDGA (Oak Ridge) from 2.1 mol/L HNO_3. Experimental details see Figure 28.

This project has received funding from the EURATOM research and training programme 2014–2018 under grant agreement No. 755171. The content of this deliverable reflects only the authors' view. The European Commission is not responsible for any use that may be made of the information it contains.

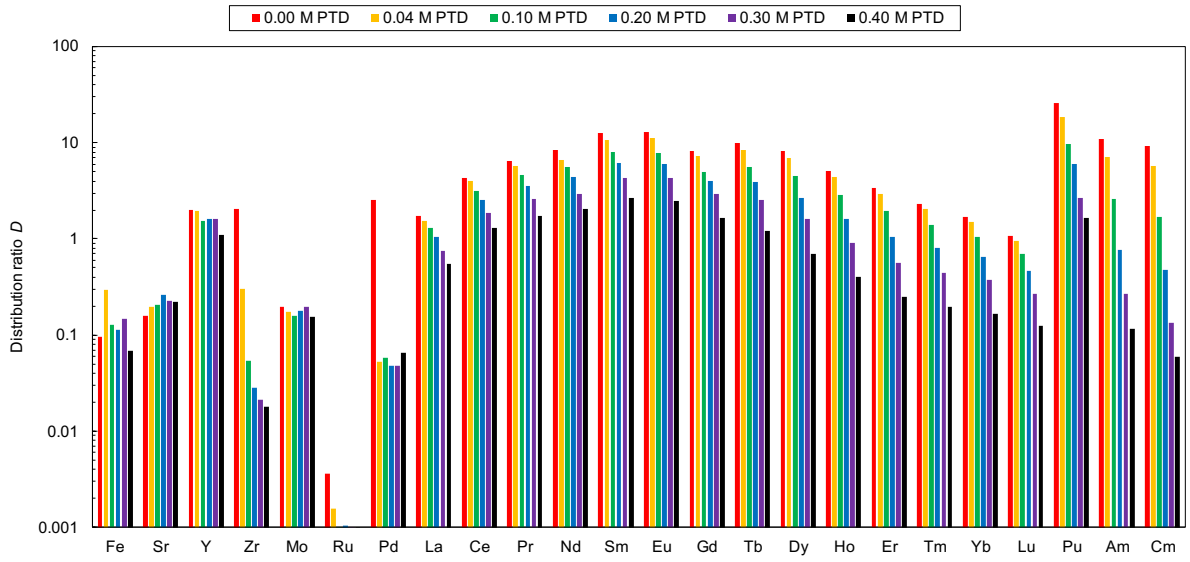

Figure 30. Distribution ratios D as a function of the PTD concentration for extraction with 0.4 mol/L *cis*-mTDDGA (Oak Ridge) from 2.1 mol/L HNO_3. Experimental details see Figure 28.

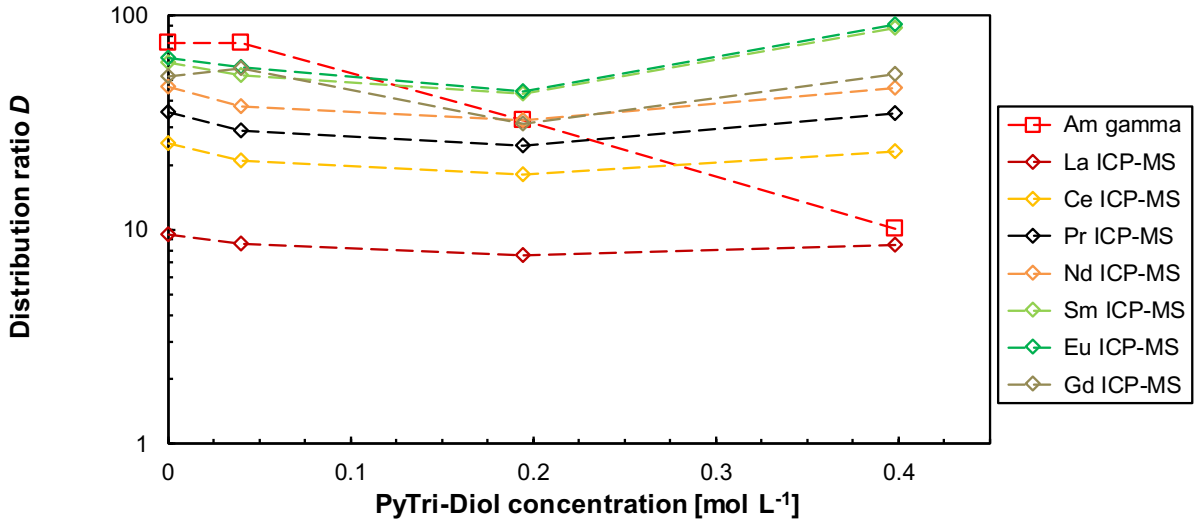

Figure 31. Distribution ratios *D* as a function of the PTD concentration for extraction with 0.4 mol/L *cis*-mTDDGA (Oak Ridge) from 3.7 mol/L HNO_3. Organic phase, 0.4 mol/L *cis*-mTDDGA (Oak Ridge) in *n*-dodecane. Aqueous phase, 10^{-5} mol/L Ln and FP in 3.7 mol/L HNO_3, spiked with ^{152}Eu, ^{239}Pu, ^{241}Am, and ^{244}Cm. 22°C, 2,220 rpm, 15 min.

CHON MODIFIERS TO IMPROVE An(III) STRIPPING FROM TODGA SOLVENTS

CHON ligands for selective An(III) stripping such as PTD[25] exhibit a lower selectivity for An(III) over light Ln(III) compared to SO_3-Ph-BTP.[15] Lipophilic modifiers were tested to increase this selectivity. The concept is that such modifiers would coordinate to coordinatively unsaturated TODGA complexes in a way that increases the extractability of light Ln(III) to a greater extent than the extractability of An(III), due to the slightly larger ionic radii of the former allowing for up to tenfold coordination.

This project has received funding from the EURATOM research and training programme 2014–2018 under grant agreement No. 755171. The content of this deliverable reflects only the authors' view. The European Commission is not responsible for any use that may be made of the information it contains.

This assumption, based solely on geometrical factors, was tested experimentally. In order to avoid stronger complexation of An(III) compared to e. g. Eu(III) by N-donor ligands, the choice of potential modifiers was limited to O-donor ligands.

RESULTS AND DISCUSSION

The experiments included radiometric determinations of the distribution ratios, *D*, of Am(III), La(III) and Eu(III) as a function of the concentration of the modifiers tested. the solvent extraction system was 1 mol/L HNO_3 / 0.2 mol/L TODGA (with or without 5% 1-octanol) in kerosene, spiked with ^{241}Am(III), ^{152}Eu(III) and ^{140}La(III).

ACETOPHENONE

The first potential modifier, acetophenone (AP, Figure 32), a liquid miscible with the kerosene diluent, was tested already within the SACSESS project. In the two-phase system: 0.2 mol/L TODGA + 0–8 mol/L AP in kerosene / 0.5 mol/L HNO_3, D_{Eu} was practically constant in the whole range of AP concentrations, while D_{La} increased with increasing AP concentration. The separation factor, $SF_{Eu/La} = D_{Eu}/D_{La}$, decreased from 26 (with no AP) to 3 (at 8 mol/L AP). Unexpectedly, however, as the AP concentration increased, D_{Am} increased almost parallel to D_{La} (Figure 33). Consequently, the corresponding separation factor did not decrease but remained almost constant at $SF_{Am/Ln} \approx 5$.[28]

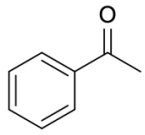

Figure 32. Acetophenone.

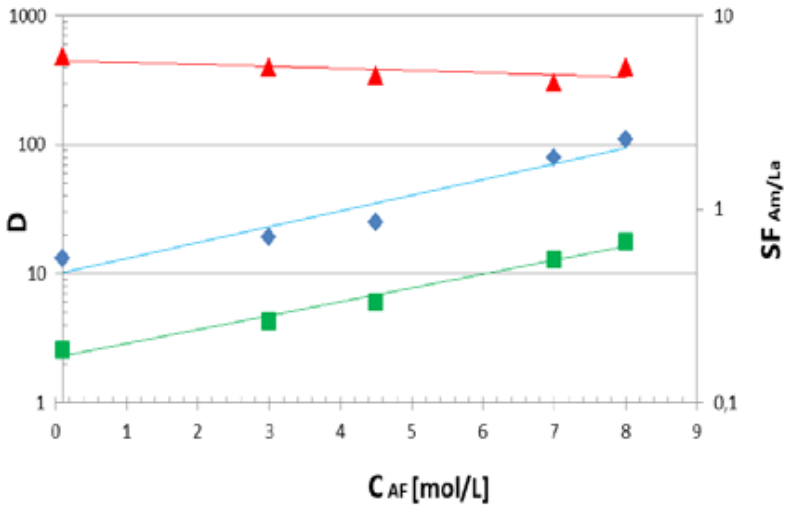

Figure 33. Dependence of the La(III) and Am(III) distribution ratios and separation factor on the concentration of acetophenone (AF). Organic phase, 0.2 mol/L TODGA + 0–8 mol/L acetophenone in kerosene. Aqueous phase, 0.5 mol/L HNO_3. ♦ – D_{Am}, ■ – D_{La}, ▲– $SF_{Am/La}$ [28]

This project has received funding from the EURATOM research and training programme 2014–2018 under grant agreement No. 755171. The content of this deliverable reflects only the authors' view. The European Commission is not responsible for any use that may be made of the information it contains.

In terms of the "geometrical" assumption, this unexpected result may be interpreted as due to a small bite angle of the monodentate AP modifier, which allows the access of the donor C=O group to the inner coordination sphere of the two central metal cations, Am^{3+} and La^{3+}, in their 1:3 TODGA complexes. Therefore, in order to hinder the coordination of the modifier molecule by the smaller Am^{3+} cation in the TODGA complex, bidentate ligands were tested.

BIDENTATE MODIFIERS

Initially, selected derivatives of 1,3,5-triazine and of benzoic acid were tested. Due to their fairly large bite angles, these ligands are expected to meet a steric hindrance to their entry into the inner coordination sphere of the Am^{3+} cation, thus exerting a weaker synergistic effect on the extraction of Am^{3+} than on the extraction of the larger La^{3+} cation. The results are shown in Table 3.

Table 3. Effect of modifiers on distribution ratios and separation factors of La(II), Eu(III) and Am(III). Organic phase, 0.2 mol/L TODGA + 0.01 mol/L modifier in 70 vol % 1-octanol/kerosene diluent. Aqueous phase, 1 mol/L HNO_3. [28]

Modifier	D_{La}	D_{Eu}	D_{Am}	$SF_{Eu/La}$	$SF_{Am/La}$
2,4,6-tri(2-pyridyl)-1,3,5-triazine	36	55	120	1.5	3.3
2,4,6-tris-(allyloxy)-1,3,5-triazine	24	59	110	2.5	4.6
benzoic acid	22	58	105	2.6	4.7
p-chlorobenzoic acid	23	67	110	2.9	4.8
p-methylbenzoic acid	25	66	102	2.6	4.1
p-aminobenzoic acid	49	64	149	1.3	3.0
No modifier	15	110	63	7.3	4.2

Unexpectedly, as in the case of the monodentate AP ligand, the modifiers tested exerted nearly parallel synergistic effects on the extraction of Am(III) and La(III). Two of them, 2,4,6-tri(2-pyridyl)-1,3,5-triazine and *p*-aminobenzoic acid, caused a small decrease in the $SF_{Am/La}$ value. Unfortunately, poor solubility of all these solid ligands in kerosene limited their concentration in the systems studied to approximately 0.01 mol/L, which made it impossible to achieve a better result. In view of that, research was focused on bidentate ligands which are either liquids under normal conditions or solids with low melting points.

Such a bidentate ligand with a large bite angle is, for example, tropolone (Figure 34), which forms five-membered rings with d-block metal ions.[29] However, the distribution ratios of La(III) in the system 0.2 mol/L TODGA + 0.01–0.05 mol/L tropolone in kerosene / 1 mol/L HNO_3 did not significantly differ from that determined in the system without tropolone.

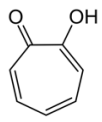

Figure 34. Tropolone.

This project has received funding from the EURATOM research and training programme 2014–2018 under grant agreement No. 755171. The content of this deliverable reflects only the authors' view. The European Commission is not responsible for any use that may be made of the information it contains.

Subsequently, butyl acetate was tested. Its presence at high concentrations up to 7 mol/L in the organic phase (0.2 mol/L TODGA in kerosene) noticeably improved extraction of La(III) from 1 mol/L HNO_3, while only slightly the extraction of Am(III) (Figure 35) and Eu(III). However, the value of $SF_{Am/La}$ = 5.0 at 7 mol/L butyl acetate (93 vol%) in kerosene is still not satisfactory.

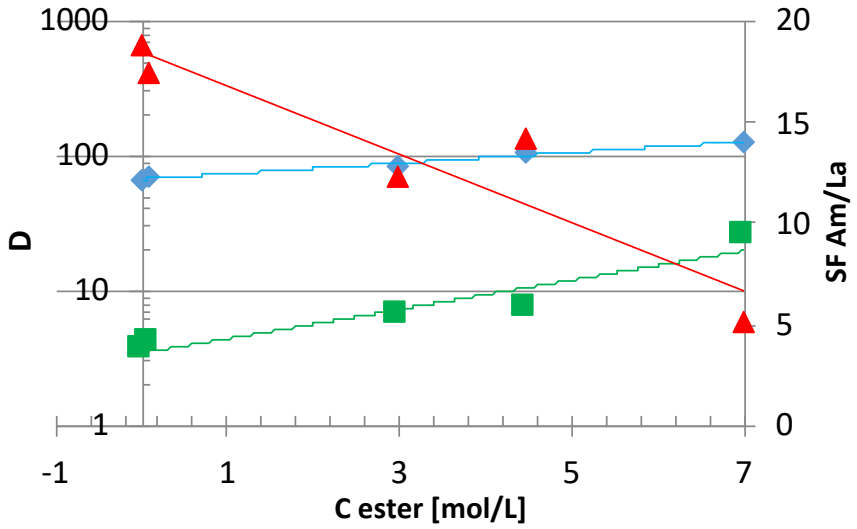

Figure 35. Dependence of distribution ratios of Am(III) (blue diamonds) and La(III) (green squares), and of the separation factor, $SF_{Am/La}$ (red triangles) on the butyl acetate concentration (0 – 7 M). Organic phase, 0.2 mol/L TODGA + 0–7 molo/L butyl acetate in kerosene. Aqueous phase, 1 mol/LHNO_3.

The other bidentate CHON ligands tested as modifiers are MHB (methyl 2-hydroxybenzoate), MAB (methyl 2-aminobenzoate) and EAB (ethyl 4-(dimethylamino)benzoate) (Figure 36).

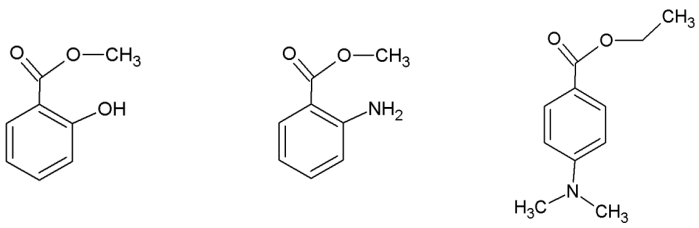

Figure 36. MHB, MAB and EAB (left to right).

These three modifiers were tested for a wide range of modifier and HNO_3 concentrations (Table 4). The organic phase was 0.2 mol/L TODGA + 5 vol % 1-octanol in kerosene, with or without the modifiers.

This project has received funding from the EURATOM research and training programme 2014–2018 under grant agreement No. 755171. The content of this deliverable reflects only the authors' view. The European Commission is not responsible for any use that may be made of the information it contains.

Table 4.Effect of modifiers, MHB, MAB and EAB on the separation factors, $SF_{Am/La}$. Organic phase, 0.2 mol/L TODGA + 0–2 mol/L modifier in kerosene. Aqueous phase, 0.1–1.0 mol/L HNO_3 concentrations.

$[HNO_3]$, mol/L	$SF_{Am/La}$		
	[MHB] 0 → 0.5 →2 mol/L	[MAB] 0 → 0.5 →2 mol/L	[EAB] 0 → 0.33 mol/L
0.1	6.8 → 6.4 → 5.3	6.8 → 11.1 → 8.5	6.8 → 6.3
0.3	6.8 → 6.1 → 5.1	6.8 → 9.9 → 8.4	6.8 → 6.3
0.5	8.5 → — → 5.8	8.5 → — → 7.8	8.5 → 6.8
0.8	9.0 → — → 6.1	9.0 → — → 8.2	9.0 → 8.3
1.0	12.5 → 13.4 → 10.6	12.5 → 10.0 → 7.7	12.5 → 9.4

Unexpected relationships between the D_M values and the modifier concentrations were observed. All these modifiers exert a weak anti-synergistic effect on metal ion extraction. The best results were obtained for MHB, see Figure 37. Both D_{Am} and D_{La} values decrease with increasing concentration of MHB in the whole range studied. Weak maxima were observed for moderate concentrations of MAB and EAP at the lowest HNO_3 concentrations studied.

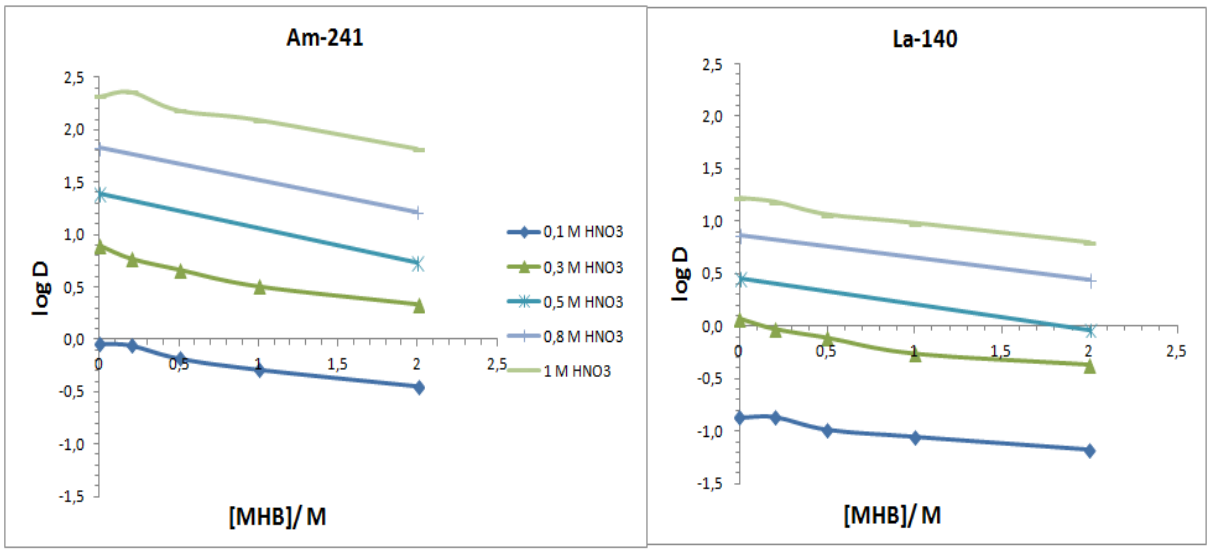

Figure 37. Dependencies of D_{Am} and D_{La} values on the MHB concentration. Organic phase, 0.2 mol/L TODGA + 0–2 mol/L MHB in kerosene. Aqueous phase, 0.1–1 mol/L HNO_3.

Nonetheless, all of these ester modifiers advantageously decrease the $SF_{Am/La}$ values with their increasing concentrations, though all these effects are small (Table 4). The greatest decrease in the $SF_{Am/La}$ value has been observed for ethyl 2-hydroxybenzoate (MHB). The magnitudes of these anti-synergistic effects are comparable to the magnitudes of the synergistic effects exerted by butyl acetate over the same concentration range. The increase in the HNO_3 concentration from 0.1 mol/L to 1.0 mol/L significantly increases the D values of both metal ions but also unfavourably increases the $SF_{Am/La}$ values.

This project has received funding from the EURATOM research and training programme 2014–2018 under grant agreement No. 755171. The content of this deliverable reflects only the authors' view. The European Commission is not responsible for any use that may be made of the information it contains.

The slight variability of the $SF_{Am/La}$ values observed for various modifiers shows that the assumption about the exclusive role of the geometry of the metal complexes in the extraction process was an oversimplification. The other factor may be a different electron transfer from the donor oxygen atoms in the modifier ligands to the acceptor orbitals of the metal ions – greater to the 6*d* of Am^{3+} than to the 5*d* of La^{3+}. That is due to a greater overlap of the former than of the latter with the lone pair orbitals of the donor oxygen atoms in the ligand, because of a greater spatial range of the 6*d* orbital. A similar conclusion has been formulated earlier, related to the 6*d*(Am^{3+}) and 5*d*(Eu^{3+}) orbitals.[30]

DMDBTDMA

To complete the present studies, a malonamide ligand having a large bite angle, *N,N*'-dimethyl-*N,N*'-dibutyltetradecylmalonamide (DMDBTDMA, Figure 38), expected to form six-membered rings with the metal ions considered, was tested as the modifier of their extraction by TODGA. The effect of the DMDBTDMA concentration on the distribution ratios of Am(III), Eu(III) and La(III) is shown in Figure 39.

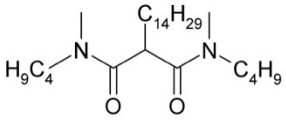

Figure 38. DMDBTDMA.

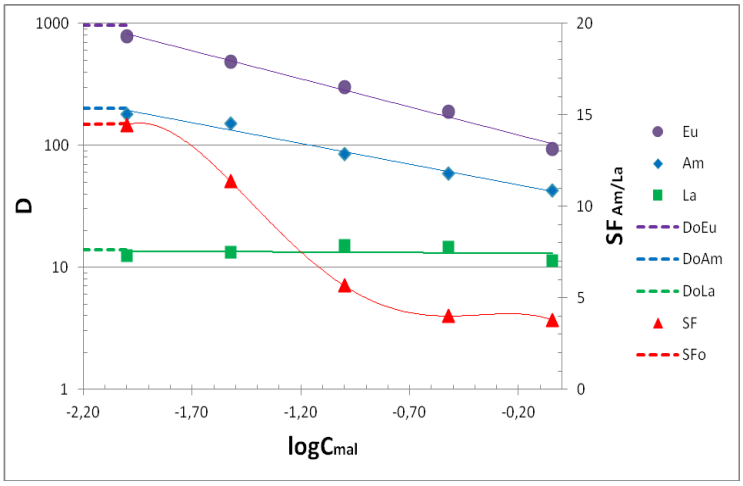

Figure 39. Dependence of the distribution ratios, *D*, of Am(III), Eu(III) and La(III) and of the separation factor, $SF_{Am/La}$ on the concentration of DMDBTDMA. Organic phase, 0.2 mol/L TODGA + 0–0.9 mol/L DMDBTDMA in kerosene. Aqueous phase, 1 mol/L HNO_3. Short broken horizontal lines on the D-axis denote the respective D_0 values (with no DMDBTDMA).

Quite unexpectedly, like in the case of the esters of aminobenzoic and hydroxybenzoic acids, the D_{Am} and D_{Eu} values decreased with increasing concentration of the modifier tested. Therefore, this bidentate diamide ligand forming six-membered rings with the metal ions studied exerts weak anti-synergistic effects on the extraction of Eu(III) and Am(III) but does not affect the D_{La} value. The reason for this behaviour may be the competition for the metal cations between the tridentate extractant TODGA and the bidentate malonamide modifier. The exchange of the two neutral ligands, TODGA for

This project has received funding from the EURATOM research and training programme 2014–2018 under grant agreement No. 755171. The content of this deliverable reflects only the authors' view. The European Commission is not responsible for any use that may be made of the information it contains.

DMDBTDMA, in the inner coordination sphere of the central metal ions in the extracted complexes, progressing with increasing DMDBTDMA concentration, may lead to decomposition of the extracted 1:3 TODGA complexes and formation of less extractable heteroleptic complexes of each metal ion with both ligands. The D_{Am} and D_{Eu} values decrease with increasing concentration of the modifier, probably because DMDBTDMA is a much less effective extractant than TODGA. In fact, Am(III) is noticeably extracted by DMDBTDMA from aqueous solutions only at high (4–5 mol/L) HNO_3 concentrations.[31] The reason of the lack of a similar anti-synergistic effect in the extraction of La(III) is unclear yet.

The value $SF_{Am/La} \leq 4$, achieved at $C_{mal} > 0.2$ mol/L in the system studied, is too high to consider it satisfactory. However, it is significantly lower than $SF_{Am/La} \approx 14$ determined in the same system with no DMDBTDMA. Nevertheless, such a decrease may be sufficient to further improve the reported[27] separation of these two metal ions when stripping Am(III) from 0.2 mol/L TODGA + 5 vol.% 1-octanol in TPH by PTD at HNO_3 concentrations above 0.5 mol/L. Moreover, there is no need to introduce additional changes to the EURO-GANEX process, which uses a mixture of two extractants, 0.2 mol/L TODGA and 0.5 mol/L DMDOHEMA (Figure 2), because the latter is chemically similar to DMDBTDMA. Indeed, $SF_{Am/La} \approx 3$ for the EURO-GANEX solvent,[32] which is close to the results obtained with ≥ 0.5 mol/L DMDBTDMA (see Figure 39).

CONCLUSION

In the EURO-GANEX process, DMDOHEMA is used as a modifier to ensure a high Pu(IV) loading capacity.[6] The present work indicates a possible additional role of this ligand in the process, i. e. facilitating the separation of Am(III) from light Ln(III) when stripping Am(III) with PTD or other novel CHON stripping agents.

PTEH

PTEH (2,6-bis[1-(2-ethylhexyl)-1,2,3-triazol-4-yl]pyridine, Figure 40)[33-34] was developed and synthesised as a potential extracting agent for the separation of An(III) from Ln(III) in a SANEX process. It may also be used in a modified CHALMEX[35] process for TRU co-separation. Compared to the current SANEX reference extracting agent, $CyMe_4$-BTBP (6,6'-bis(5,5,8,8-tetramethyl-5,6,7,8-tetrahydro-benzo-1,2,4-triazin-3-yl)-2,2'-bipyridine),[36] PTEH has advantageous properties such as better solubility and faster kinetics.

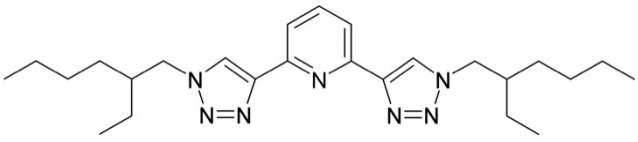

Figure 40. PTEH.

A batch of PTEH was synthesised[33-34] and further distribution data for the extraction of HNO_3, Pu(IV), Am(III) and Ln(III) were determined.

This project has received funding from the EURATOM research and training programme 2014–2018 under grant agreement No. 755171. The content of this deliverable reflects only the authors' view. The European Commission is not responsible for any use that may be made of the information it contains.

NITRIC ACID EXTRACTION

The distribution of nitric acid between 0.5–5 mol/L HNO_3 and solvents containing 0.1–0.3 mol/L PTEH + 10% vol. 1-octanol in TPH was measured, and a simple equilibrium model was established.

Third phase formation was observed for 0.3 mol/L PTEH and initial aqueous nitric acid concentrations ≥ 4 mol/L but not for 0.1–0.2 mol/L PTEH. This is unexpected since generally, loading capacity is increasing with increasing extracting agent concentration.

Figure 41 shows distribution data for nitric acid extraction into 0.1–0.3 mol/L PTEH + 10% vol. 1-octanol in TPH. Organic phase nitric acid concentrations exceeding the PTEH concentrations indicate the formation of 2:1 adducts, $(HNO_3)_2 \cdot$PTEH.

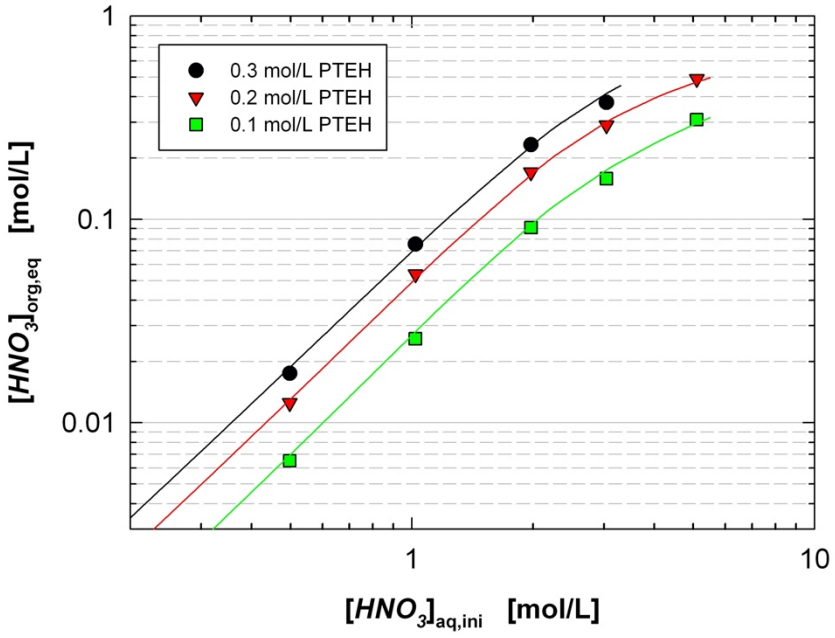

Figure 41. Extraction of HNO_3 into PTEH. Aqueous phase, HNO_3. Organic phase, PTEH + 10% vol. 1-octanol in TPH. *O/A* = 1, *T* = 20 °C. Symbols, experimental. Lines, calculated.

Nitric acid extraction was calculated accounting for its extraction both by 1-octanol[12] and by PTEH. The extraction by 1-octanol was calculated along the formation of the 1:2 adduct, $HNO_3 \cdot (OctOH)_2$ with the respective constant, K_{OctOH} = 0.0115, as described in the literature.[12]

The extraction by PTEH was calculated accounting for the 1:1 and 2:1 adducts, $(HNO_3)_n \cdot$PTEH (n = 1, 2) with the respective extraction constants,

$$K_{11} = \frac{[(HNO_3)L]}{(H^+) \cdot (NO_3^-) \cdot [L]} = 0.5$$

This project has received funding from the EURATOM research and training programme 2014–2018 under grant agreement No. 755171. The content of this deliverable reflects only the authors' view. The European Commission is not responsible for any use that may be made of the information it contains.

$$K_{21} = \frac{[(HNO_3)_2L]}{(H^+)^2 \cdot (NO_3^-)^2 \cdot [L]} = 0.07$$

Aqueous phase activities were calculated with the Specific Ion Interaction Theory (SIT)[37-38] as described in reference.[12]

The model agrees well with the experiments, see Figure 41.

EXTRACTION OF ACTINIDES AND LANTHANIDES

The extraction of Pu(IV), Am(III), and Ln(III) into solvents containing PTEH in modified TPH is shown in Figure 42 (0.1 mol/L PTEH + 10% vol. 1-octanol in TPH), Figure 43 (0.2 mol/L PTEH + 10% vol. 1-octanol in TPH), and Figure 44 (0.3 mol/L PTEH + 10% vol. 1-octanol in TPH). Further to the distribution ratios measured by ICP-MS, Figure 43 shows ^{241}Am(III) and ^{154}Eu(III) distribution data measured by gamma spectrometry. ICP-MS and gamma data are in good agreement.

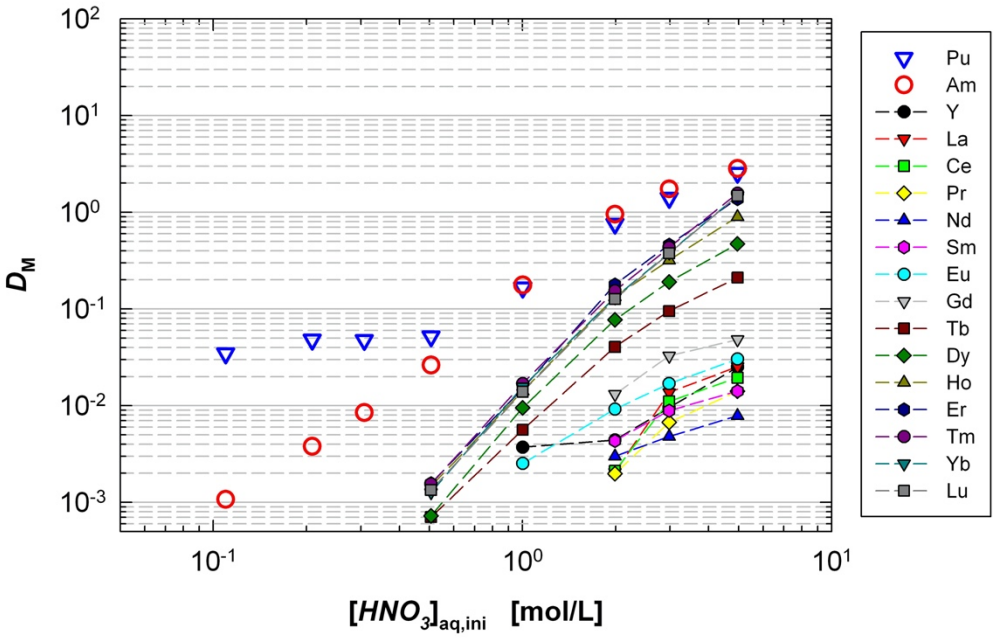

Figure 42. Extraction of Pu(IV), Am(III), Ln(III) and Y(III) into 0.1 mol/L PTEH + 10% vol. 1-octanol in TPH. Aqueous phase, ^{239}Pu(IV), ^{243}Am(III), Y(III), La(III)–Lu(III) each 1 mg/L in HNO_3. *O/A* = 1, *T* = 20 °C.

With a PTEH concentration of 0.2 mol/L (which is the reference concentration[33-34]) and nitric acid concentrations in the range of 1–3 mol/L, Pu(IV) and Am(III) are extracted ($D > 1$), and distribution ratios of all "fission lanthanides" (La(III)–Dy(III) + Y(III)) are below 1. Pu(IV) and Am(III) can be stripped (i. e. $D < 1$) for $[HNO_3] < 0.3$ mol/L.

Independent of the PTEH concentration, Pu(IV) distribution ratios plateau at a lower value of $D_{Pu} \approx 0.03$. Other than that, Pu(IV) and Am(III) show similar distribution ratios. The selectivity for Am(III) over Eu(III) is $SF_{Am/Eu} \approx 100$.

This project has received funding from the EURATOM research and training programme 2014–2018 under grant agreement No. 755171. The content of this deliverable reflects only the authors' view. The European Commission is not responsible for any use that may be made of the information it contains.

The distribution ratios reported here are slightly greater than those reported in references.[33-34] The Ln(III) pattern is similar to that reported in reference.[34]

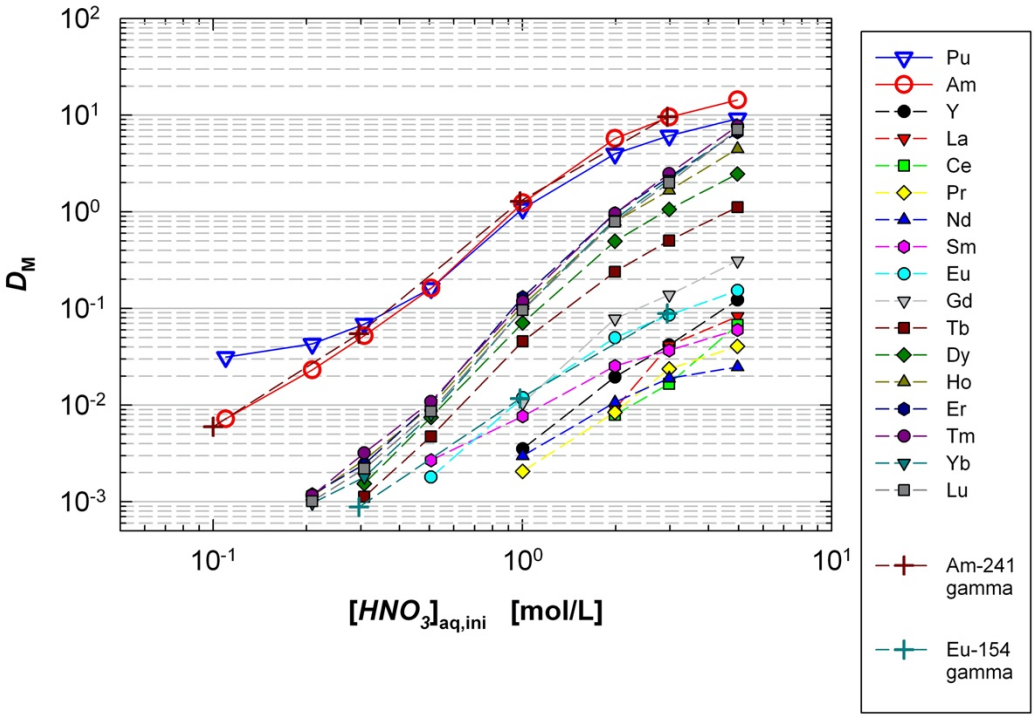

Figure 43. Extraction of Pu(IV), Am(III), Ln(III) and Y(III) into 0.2 mol/L PTEH + 10% vol. 1-octanol in TPH. Aqueous phase, [^{239}Pu(IV), ^{243}Am(III), Y(III), La(III)–Lu(III) each 1 mg/L] or [^{241}Am(III) + ^{154}Eu(III) each 1 kBq/mL] in HNO_3. *O/A* = 1, *T* = 20 °C.

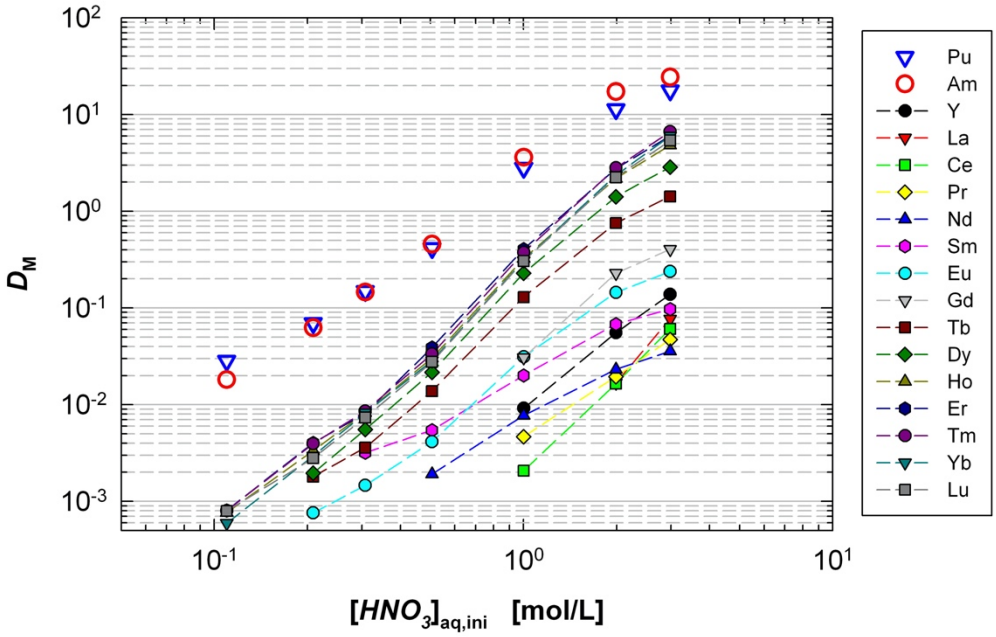

Figure 44. Extraction of Pu(IV), Am(III), Ln(III) and Y(III) into 0.3 mol/L PTEH + 10% vol. 1-octanol in TPH. Aqueous phase, ^{239}Pu(IV), ^{243}Am(III), Y(III), La(III)–Lu(III) each 1 mg/L in HNO_3. *O/A* = 1, *T* = 20 °C.

This project has received funding from the EURATOM research and training programme 2014–2018 under grant agreement No. 755171. The content of this deliverable reflects only the authors' view. The European Commission is not responsible for any use that may be made of the information it contains.

REFERENCES

1. Sasaki, Y.; Sugo, Y.; Suzuki, S.; Tachimori, S., The novel extractants, diglycolamides, for the extraction of lanthanides and actinides in HNO_3/*n*-dodecane system. *Solvent Extr. Ion Exch.* **2001,** *19* (1), 91–103.

2. Ansari, S. A.; Pathak, P. N.; Manchanda, V. K.; Husain, M.; Prasad, A. K.; Parmar, V. S., *N,N,N',N'*-tetraoctyl diglycolamide (TODGA): a promising extractant for actinide partitioning from high-level waste (HLW). *Solvent Extr. Ion Exch.* **2005,** *23* (4), 463–479.

3. Whittaker, D.; Geist, A.; Modolo, G.; Taylor, R.; Sarsfield, M.; Wilden, A., Applications of diglycolamide based solvent extraction processes in spent nuclear fuel reprocessing, part 1: TODGA. *Solvent Extr. Ion Exch.* **2018,** *36* (3), 223–256.

4. Taylor, R.; (ed.), *Reprocessing and Recycling of Spent Nuclear Fuel*. Woodhead Publishing: Cambridge, UK, 2015.

5. Geist, A.; Adnet, J.-M.; Bourg, S.; Ekberg, C.; Galán, H.; Guilbaud, P.; Miguirditchian, M.; Modolo, G.; Rhodes, C.; Taylor, R., An overview of solvent extraction processes developed in Europe for advanced nuclear fuel recycling, part 1 — heterogeneous recycling. *Separ. Sci. Technol.* **2020,** *DOI: 10.1080/01496395.2020.1795680*.

6. Brown, J.; McLachlan, F.; Sarsfield, M.; Taylor, R.; Modolo, G.; Wilden, A., Plutonium loading of prospective grouped actinide extraction (GANEX) solvent systems based on diglycolamide extractants. *Solvent Extr. Ion Exch.* **2012,** *30* (2), 127–141.

7. Carrott, M. J.; Gregson, C. R.; Taylor, R. J., Neptunium extraction and stability in the GANEX solvent: 0.2 M TODGA/0.5 M DMDOHEMA/kerosene. *Solvent Extr. Ion Exch.* **2013,** *31* (5), 463–482.

8. Carrott, M.; Bell, K.; Brown, J.; Geist, A.; Gregson, C.; Hérès, X.; Maher, C.; Malmbeck, R.; Mason, C.; Modolo, G.; Müllich, U.; Sarsfield, M.; Wilden, A.; Taylor, R., Development of a new flowsheet for co-separating the transuranic actinides: the "EURO-GANEX" process. *Solvent Extr. Ion Exch.* **2014,** *32* (5), 447–467.

9. Carrott, M.; Geist, A.; Hérès, X.; Lange, S.; Malmbeck, R.; Miguirditchian, M.; Modolo, G.; Wilden, A.; Taylor, R., Distribution of plutonium, americium and interfering fission products between nitric acid and a mixed organic phase of TODGA and DMDOHEMA in kerosene, and implications for the design of the "EURO-GANEX" process. *Hydrometallurgy* **2015,** *152*, 139–148.

10. Malmbeck, R.; Magnusson, D.; Bourg, S.; Carrott, M.; Geist, A.; Hérès, X.; Miguirditchian, M.; Modolo, G.; Müllich, U.; Sorel, C.; Taylor, R.; Wilden, A., Homogenous recycling of transuranium elements from irradiated fast reactor fuel by the EURO-GANEX solvent extraction process. *Radiochim. Acta* **2019,** *107* (9–11), 917–929.

11. Woodhead, D.; McLachlan, F.; Taylor, R.; Müllich, U.; Geist, A.; Wilden, A.; Modolo, G., Nitric acid extraction into a TODGA solvent modified with 1-octanol. *Solvent Extr. Ion Exch.* **2019,** *37* (2), 173–190.

12. Geist, A., Extraction of nitric acid into alcohol:kerosene mixtures. *Solvent Extr. Ion Exch.* **2010,** *28* (5), 596–607.

13. Berthon, L.; Morel, J. M.; Zorz, N.; Nicol, C.; Virelizier, H.; Madic, C., DIAMEX process for minor actinide partitioning: hydrolytic and radiolytic degradations of malonamide extractants. *Separ. Sci. Technol.* **2001,** *36* (5–6), 709–728.

14. Geist, A.; Berthon, L.; Charbonnel, M.-C.; Müllich, U., Extraction of nitric acid, americium(III), curium(III), and lanthanides(III) into DMDOHEMA dissolved in kerosene. *Solvent Extr. Ion Exch.* **2020,** *38* (7), 681–702.

This project has received funding from the EURATOM research and training programme 2014–2018 under grant agreement No. 755171. The content of this deliverable reflects only the authors' view. The European Commission is not responsible for any use that may be made of the information it contains.

15. Geist, A.; Müllich, U.; Magnusson, D.; Kaden, P.; Modolo, G.; Wilden, A.; Zevaco, T., Actinide(III)/lanthanide(III) separation via selective aqueous complexation of actinides(III) using a hydrophilic 2,6-bis(1,2,4-triazin-3-yl)-pyridine in nitric acid. *Solvent Extr. Ion Exch.* **2012,** *30* (5), 433–444.

16. Madic, C.; Hudson, M. J. *High-level liquid waste partitioning by means of completely incinerable extractants*; EUR 18038, European Commission, Luxembourg: 1998.

17. Iqbal, M.; Huskens, J.; Verboom, W.; Sypula, M.; Modolo, G., Synthesis and Am/Eu extraction of novel TODGA derivatives. *Supramolec. Chem.* **2010,** *22* (11/12), 827–837.

18. Wilden, A.; Modolo, G.; Lange, S.; Sadowski, F.; Beele, B. B.; Skerencak-Frech, A.; Panak, P. J.; Iqbal, M.; Verboom, W.; Geist, A.; Bosbach, D., Modified diglycolamides for the An(III) + Ln(III) co-separation: evaluation by solvent extraction and time-resolved laser fluorescence spectroscopy. *Solvent Extr. Ion Exch.* **2014,** *32* (2), 119–137.

19. Wilden, A.; Kowalski, P. M.; Klaß, L.; Kraus, B.; Kreft, F.; Modolo, G.; Li, Y.; Rothe, J.; Dardenne, K.; Geist, A.; Leoncini, A.; Huskens, J.; Verboom, W., Unprecedented inversion of selectivity and extraordinary difference in the complexation of trivalent f elements by diastereomers of a methylated diglycolamide. *Chem. Eur. J.* **2019,** *25* (21), 5507–5513.

20. Malmbeck, R.; Magnusson, D.; Geist, A., Modified diglycolamides for grouped actinide separation. *J. Radioanal. Nucl. Chem.* **2017,** *314* (3), 2531–2538.

21. Siddall, T. H.; Dukes, E. K., Kinetics of HNO2 Catalyzed Oxidation of Neptunium(V) by Aqueous Solutions of Nitric Acid1. *J Am Chem Soc* **1959,** *81* (4), 790-794.

22. Wilden, A.; Kowalski, P. M.; Klaß, L.; Kraus, B.; Kreft, F.; Modolo, G.; Li, Y.; Rothe, J.; Dardenne, K.; Geist, A.; Leoncini, A.; Huskens, J.; Verboom, W., Unprecedented Inversion of Selectivity and Extraordinary Difference in the Complexation of Trivalent *f*-Elements by Diastereomers of a Methylated Diglycolamide. *Chem. Eur. J.* **2019,** *25* (21), 5507-5513.

23. Sypula, M.; Wilden, A.; Schreinemachers, C.; Malmbeck, R.; Geist, A.; Taylor, R.; Modolo, G., Use of polyaminocarboxylic acids as hydrophilic masking agents for fission products in actinide partitioning processes. *Solvent Extr. Ion Exch.* **2012,** *30* (7), 748–764.

24. Weigl, M.; Geist, A.; Müllich, U.; Gompper, K., Kinetics of americium(III) extraction and back extraction with BTP. *Solvent Extr. Ion Exch.* **2006,** *24* (6), 845–860.

25. Macerata, E.; Mossini, E.; Scaravaggi, S.; Mariani, M.; Mele, A.; Panzeri, W.; Boubals, N.; Berthon, L.; Charbonnel, M.-C.; Sansone, F.; Arduini, A.; Casnati, A., Hydrophilic clicked 2,6-bis-triazolyl-pyridines endowed with high actinide selectivity and radiochemical stability: toward a closed nuclear fuel cycle. *J. Amer. Chem. Soc.* **2016,** *138* (23), 7232–7235.

26. Wagner, C.; Mossini, E.; Macerata, E.; Mariani, M.; Arduini, A.; Casnati, A.; Geist, A.; Panak, P. J., Time-resolved laser fluorescence spectroscopy study of the coordination chemistry of a hydrophilic CHON [1,2,3-triazol-4-yl]pyridine ligand with Cm(III) and Eu(III). *Inorg. Chem.* **2017,** *56* (4), 2135–2144.

27. Mossini, E.; Macerata, E.; Wilden, A.; Kaufholz, P.; Modolo, G.; Iotti, N.; Casnati, A.; Geist, A.; Mariani, M., Optimization and single-stage centrifugal contactor experiments with the novel hydrophilic complexant PyTri-Diol for the i-SANEX process. *Solvent Extr. Ion Exch.* **2018,** *36* (4), 373–386.

28. Narbutt, J.; Herdzik-Koniecko, I.; Rejnis-Strzelak, M. *The use of synergistic effects of lipophilic modifiers of TODGA-containing organic phase for improving separation of americium(III) from the early lanthanides in the*

This project has received funding from the EURATOM research and training programme 2014–2018 under grant agreement No. 755171. The content of this deliverable reflects only the authors' view. The European Commission is not responsible for any use that may be made of the information it contains.

process of stripping the metals with hydrophilic ligands. A novel concept for solving the problem; Raport IChTJ, Seria B nr 2/2017, Warszawa 2017.

29. Narbutt, J.; Czerwiński, M.; Krejzler, J., Seven-coordinate d0 and d10 ions − computational and experimental studies on tris(tropolonato)metal(III)−TOPO adducts. *Eur. J. Inorg. Chem.* **2001,** *2001* (12), 3187–3197.

30. Narbutt, J.; Wodynski, A.; Pecul, M., The selectivity of diglycolamide (TODGA) and bis-triazine-bipyridine (BTBP) ligands in actinide/lanthanide complexation and solvent extraction separation – a theoretical approach. *Dalton Trans.* **2015,** *44*, 2657–2666.

31. Nigond, L.; Condamines, N.; Cordier, P. Y.; Livet, J.; Madic, C.; Cuillerdier, C.; Musikas, C.; Hudson, M. J., Recent advances in the treatment of nuclear wastes by the use of diamide and picolinamide extractants. *Separ. Sci. Technol.* **1995,** *30* (7–9), 2075–2099.

32. Bell, K.; Carpentier, C.; Carrott, M.; Geist, A.; Gregson, C.; Hérès, X.; Magnusson, D.; Malmbeck, R.; McLachlan, F.; Modolo, G.; Müllich, U.; Sypula, M.; Taylor, R.; Wilden, A., Progress towards the development of a new GANEX process. *Proc. Chem.* **2012,** *7*, 392–397.

33. Ossola, A.; Macerata, E.; Mossini, E.; Giola, M.; Gullo, M. C.; Arduini, A.; Casnati, A.; Mariani, M., 2,6-Bis(1-alkyl-1H-1,2,3-triazol-4-yl)-pyridines: selective lipophilic chelating ligands for minor actinides. *J. Radioanal. Nucl. Chem.* **2018,** *318* (3), 2013–2022.

34. Ossola, A. *Development of novel extracting systems for safe transuranium elements separation from spent nuclear fuel*; PhD thesis, Politecnico di Milano: 2019.

35. Halleröd, J.; Ekberg, C.; Löfström-Engdahl, E.; Aneheim, E., Development of the Chalmers grouped actinide extraction process. *Nukleonika* **2015,** *60* (4), 829–835.

36. Geist, A.; Hill, C.; Modolo, G.; Foreman, M. R. S. J.; Weigl, M.; Gompper, K.; Hudson, M. J.; Madic, C., 6,6 '-bis (5,5,8,8-tetramethyl-5,6,7,8-tetrahydro-benzo[1,2,4]triazin-3-yl) [2,2 ']bipyridine, an effective extracting agent for the separation of americium(III) and curium(III) from the lanthanides. *Solvent Extr. Ion Exch.* **2006,** *24* (4), 463–483.

37. Ciavatta, L., The Specific Interaction Theory in evaluating ionic equilibria. *Annali Di Chimica* **1980,** *70* (11-1), 551–567.

38. Guillaumont, R.; Fanghänel, T.; Fuger, J.; Grenthe, I.; Neck, V.; Palmer, D. A.; Rand, M. H., *Chemical Thermodynamics (OECD-NEA TDB)*. Elsevier: Amsterdam, 2003; Vol. 5.

This project has received funding from the EURATOM research and training programme 2014–2018 under grant agreement No. 755171. The content of this deliverable reflects only the authors' view. The European Commission is not responsible for any use that may be made of the information it contains.